Topoisomerase I Essentiality, DnaA-independent Chromosomal Replication, and Transcription-Replication Conflict in *Escherichia coli*

J Krishna Leela[a], Nalini Raghunathan[a], and J Gowrishankar[a,b#]

[a]Laboratory of Bacterial Genetics, Centre for DNA Fingerprinting and Diagnostics, Hyderabad, India

[b]Indian Institute of Science Education and Research Mohali, SAS Nagar, India

Running Head: Topoisomerase I essentiality in *E. coli*

#Address correspondence to Dr J Gowrishankar (Orcid ID: 0000-0003-2483-9209), Tel: +91-172-2240266; Fax: +91-172-2240124; Email: shankar@iisermohali.ac.in

Keywords: DNA supercoiling, topoisomerase I, R-loops, constitutive stable DNA replication, transcription-replication conflict

Abstract

Topoisomerase I (Topo I) of *Escherichia coli*, encoded by *topA*, acts to relax negative supercoils in DNA. Topo I deficiency results in hypernegative supercoiling, formation of transcription-associated RNA-DNA hybrids (R-loops), and DnaA- and *oriC*-independent constitutive stable DNA replication (cSDR), but some uncertainty persists as to whether *topA* is essential for viability in *E. coli* and related enterobacteria. Here we show that several *topA* alleles, including Δ*topA*, confer lethality in derivatives of wild-type *E. coli* strain MG1655. Viability in absence of Topo I was restored with two perturbations, neither of which reversed the hypernegative supercoiling phenotype: (i) in a reduced-genome strain MDS42, or (ii) by an RNA polymerase (RNAP) mutation *rpoB*35* that has been reported to alleviate the deleterious consequences of RNAP backtracking and transcription-replication conflicts. Four phenotypes related to cSDR were identified for *topA* mutants: (i) One of the *topA* alleles rescued Δ*dnaA* lethality; (ii) in *dnaA*$^+$ derivatives, Topo I deficiency generated a characteristic copy number peak in the terminus region of the chromosome; (iii) *topA* was synthetically lethal with *rnhA* (encoding RNase HI, whose deficiency also confers cSDR); and (iv) *topA rnhA* synthetic lethality was itself rescued by Δ*dnaA*. We propose that the terminal lethal consequence of hypernegative DNA supercoiling in *E. coli topA* mutants is RNAP backtracking during transcription elongation and associated R-loop formation, which in turn lead to transcription-replication conflicts and to cSDR.

41 **Importance**

42 In all life forms, double helical DNA exists in a topologically supercoiled
43 state. The enzymes DNA gyrase and topoisomerase I act, respectively, to
44 introduce and to relax negative DNA supercoils in *Escherichia coli*. That gyrase
45 deficiency leads to bacterial death is well established, but the essentiality of
46 topoisomerase I for viability has been less certain. This study confirms that
47 topoisomerase I is essential for *E. coli* viability, and suggests that in its
48 absence aberrant chromosomal DNA replication and excessive transcription-
49 replication conflicts occur that are responsible for lethality.

50

Introduction

DNA in all cells is negatively supercoiled, and in bacteria such as *Escherichia coli* two enzymes gyrase and topoisomerase I (Topo I) ordinarily act oppositely to maintain the homeostasis of DNA superhelical density (reviewed in 1–4). DNA gyrase is a hetero-tetrameric enzyme (comprised of two subunits each of GyrA and GyrB proteins) that is ATP-dependent and introduces negative supercoils, whereas Topo I (encoded by *topA*) is an 865 amino acid-long monomer that catalyzes relaxation of supercoiled DNA in an energy-independent reaction. An important role for Topo I is in the dissipation of negative supercoils, in accord with the twin-domain supercoiling model (5, 6), that are generated behind RNA polymerase (RNAP) in the transcription elongation complex (TEC).

That gyrase deficiency leads to bacterial death is well established. On the other hand, the essentiality of Topo I for viability, in either *E. coli* or closely related bacteria such as *Salmonella enterica* and *Shigella flexneri*, is somewhat less certain (7–13). One difficulty has been that *topA* mutants rapidly accumulate suppressors which are often in the genes encoding the gyrase subunits (8–10, 13–17); and consistent with their opposing actions, gyrase and Topo I mutations can, in combination, partially cancel one another's sickness or inviability (18, 19). Growth of *E. coli topA* mutants is also improved upon overexpression or amplification of genes encoding the topoisomerases III (13, 18, 20) or –IV (10, 16, 19).

Topo I deficiency is associated with an increased prevalence of R-loops (RNA-DNA hybrids) in the cells, which has been attributed to re-annealing of the 5'-end of nascent RNA into hyper-negatively supercoiled DNA behind the TEC under these conditions (21–23, reviewed in 4, 24, 25). Overexpression of RNase HI (encoded by *rnhA*), which degrades RNA in RNA-DNA hybrids, can alleviate some of the phenotypes of *topA* mutants (18, 22, 23, 26–28); and conversely, *topA rnhA* mutants exhibit exacerbated sickness (13, 26, 29). In principle, R-loops can exert toxicity by acting as road-blocks to subsequent transcription (30, 31) and to replication (32–34); and a third mechanism for toxicity is by serving as sites for initiation of aberrant chromosomal

83 replication, as further outlined below. That R-loop formation is modulated by
84 DNA supercoiling has been shown also in the CRISPR-Cas9 system (35), and
85 in eukaryotic cells (36–38).

86 Recent evidence indicates that transcription-replication conflicts can
87 themselves lead to increased formation of R-loops in the genome following
88 RNAP backtracking at the sites of conflict (39–42, reviewed in 43–45). It has
89 also been suggested that extended RNAP backtracking could be associated
90 with R-loop formation from the 3'-end of the nascent RNA (40, 46).

91 R-loops are physiological initiators of ColE1 plasmid replication (47),
92 but in addition their excessive occurrence (as in *rnhA* mutants) can lead to
93 pathological initiation of chromosomal DNA replication in both bacteria
94 (reviewed in 48–50) and eukaryotes (51). Such aberrant replication in bacteria
95 is referred to as constitutive stable DNA replication (cSDR) since, unlike
96 ordinary chromosomal replication which is initiated at *oriC* with the aid of the
97 unstable protein DnaA, it continues long after inhibition of protein synthesis
98 in the cells. cSDR can be identified biochemically as persistent DNA synthesis
99 following addition of translational inhibitors such as chloramphenicol or
100 spectinomycin.

101 cSDR can also be identified genetically as rescue of lethality associated
102 with loss of DnaA function, which is a more stringent test of cSDR since it
103 demonstrates the capability to duplicate the entire chromosome in the
104 absence of *oriC*-initiated replication (48, 49). During its progression around
105 the bacterial chromosome, such aberrant replication would be expected also
106 to encounter (i) increased head-on conflicts with TECs on heavily transcribed
107 genes (especially the *rrn* operons) that have evolved to be co-directional with
108 *oriC*-initiated replisome progression, and (ii) increased arrest at *Ter* sites
109 flanking the terminus region which are bound by the Tus protein (52, 53). The
110 occurrence of cSDR in *rnhA* mutants has been established through both the
111 biochemical and the genetic assays (48). The protein DksA, which participates
112 in avoidance or resolution of transcription-replication conflicts (54, 55), is also
113 required for viability of *rnhA dnaA* mutants (56).

114 In recent work, Drolet's group has shown by the biochemical assays
115 that cSDR occurs in Topo I-deficient cells (28). Kornberg and coworkers had
116 also shown earlier that specificity for replication initiation from *oriC in vitro*
117 requires both RNase HI and Topo I (57, 58).

118 In this study, we have examined several *topA* insertion and deletion
119 alleles for both their viability and their ability to rescue Δ*dnaA* lethality in *E.*
120 *coli*. Our results indicate that *topA* null alleles are lethal in the wild-type strain
121 MG1655 but that they are viable in MDS42, which is an engineered derivative
122 lacking all prophages and transposable elements (59). The null mutants of
123 MG1655 were viable with *rpoB*35*, which encodes an RNAP variant that has
124 been reported to alleviate the deleterious effects of transcription-replication
125 conflicts(40, 52, 60–65). Both in MDS42 and with *rpoB*35*, the viable Topo I-
126 deficient derivatives continued to exhibit increased negative supercoiling. One
127 *topA* allele could also rescue Δ*dnaA* lethality, providing genetic confirmation
128 of cSDR in Topo I-deficient strains. We propose that bacterial lethality in
129 absence of Topo I is caused by RNAP backtracking during transcription
130 elongation and associated R-loop formation, which in turn then lead to
131 transcription-replication conflicts and to cSDR.

132 **Results**

133 **Description of *topA* insertion and deletion mutations and the assay to**
134 **test for their viability.** Three pairs of *topA* mutations were constructed on
135 the *E. coli* chromosome by the recombineering approach of Datsenko and
136 Wanner (66), each pair comprised of an FRT-flanked Kan^R element and the
137 corresponding derivative with Flp recombinase-mediated site-specific excision
138 of the Kan^R element to leave behind a "scar" of 27 in-frame codons; these are
139 designated below by the suffixes "::Kan" and "::FRT", respectively.

140 The three pairs of mutations represent the following (Fig. 1A): (i) deletion
141 of all but the first codon and the last six codons (860-865) of the *topA* open-
142 reading frame (Δ*topA*), that is, similar to the various gene knock-outs of the
143 Keio collection (67); (ii) insertion beyond codon 480 in *topA* (*topA*-Ins480), this
144 position being chosen because an earlier study had shown that a Tet^R

145 insertion allele at this site was viable and associated with increased frequency
146 of transposon precise excisions (11); and (iii) deletion beyond codon 480 until
147 codon 860 in *topA* (*topA*-480Δ).

148 All the *topA* mutations were constructed and maintained in derivatives
149 that were also Δ*lacZ* on the chromosome and carried a shelter plasmid
150 derivative of a single-copy-number IncW replicon encoding trimethoprim (Tp)-
151 resistance (68) with *topA*$^+$ and *lacZ*$^+$ genes. Since this plasmid's segregation
152 into daughter cells during cell division is not tightly controlled, around 10%
153 of cells in a population are plasmid-free. Only provided that these latter cells
154 are viable, they grow as white colonies on Tp-free medium supplemented with
155 Xgal, whereas the plasmid-bearing cells grow as blue colonies on these plates.
156 The appearance of white colonies which can be subsequently purified,
157 therefore, is a demonstration of viability in absence of the *topA*$^+$ shelter
158 plasmid, and we have employed the similar blue-white screening assays
159 earlier for tests of viability with other essential genes such as *rho, nusG, dnaA*,
160 and *rne* (69–71).

161 **Viability of *topA* mutations in MDS42 and MG1655 *rpoB*35*.** With the
162 blue-white assay above, we found that none of the six *topA* alleles is viable in
163 MG1655 (Fig. 1B). These observations are consistent with those of Stockum
164 et al. (13) who also employed a similar approach to conclude that *topA* is
165 essential in *E. coli.*

166 By the same blue-white assay, we could show that all the *topA*
167 mutations are viable in strain MDS42 and in *rpoB*35* derivatives of both
168 MG1655 and MDS42, on both LB and defined media (Fig. 1B and Supp. Fig.
169 S1A); the growth of white colonies of the MDS42 *topA* derivatives was
170 improved in presence of *rpoB*35*, on both media (Supp. Fig. S1B). MDS42 is
171 a derivative of MG1655 with 14% of its genome (comprising all prophages and
172 transposable elements) deleted (59), while *rpoB*35* is a mutation in RNAP that
173 has been reported to render the enzyme less prone to backtracking or arrest
174 and more accommodative of conflicts with replication (40, 52, 60–65).

175 In microscopy experiments (Supp. Fig. S2), cell size and morphology

176 were unchanged with the *rpoB*35* mutation alone in both MG1655 and
177 MDS42. Cells of the MDS42 *topA* mutant were filamented, and the
178 filamentation was to a large extent suppressed in the *topA rpoB*35* derivative.
179 The *topA rpoB*35* derivative of MG1655 was also moderately filamented.

180 Growth rate experiments in liquid cultures did not yield reliable data
181 because of extended lag times and accumulation of suppressors in the *topA*
182 derivatives. Suppressor accumulation has also been documented earlier for
183 *topA* mutants by other workers (8, 13). Based on the observation that the
184 "white" *topA* mutant clones in the blue-white screening assay grow to colonies
185 of around 10^8 cells in 48 hours, we have estimated a doubling time of around
186 100 min.

187 For reasons that are explained in the Discussion, we tested whether
188 suppression of *topA* lethality by *rpoB*35* in MG1655 is abolished in absence
189 of the UvrD DNA helicase in the cells. In the blue-white assay, viable colonies
190 of MG1655 *rpoB*35 topA* were obtained even in a Δ*uvrD* background,
191 indicating that the suppression is UvrD-independent (Supp. Fig. S3A).

192 **Rescue of *topA* lethality in MDS42 or by *rpoB*35* is not because of**
193 **reversal of hypernegative supercoiling.** Lethality caused by loss of Topo I is
194 associated with greatly elevated levels of negative supercoiling *in vivo*, and at
195 least some suppressors of inviability, such as mutations in *gyrA* or *gyrB* and
196 overexpression or amplification of genes encoding topoisomerases III or -IV,
197 also confer reversal of the hypernegative supercoiling phenotype. To examine
198 whether the viability of *topA* null mutants in MDS42 and with *rpoB*35* is
199 correlated with reversal of hypernegative supercoiling, we determined their
200 supercoiling status, by chloroquine-agarose gel electrophoresis (21, 72) of a
201 reporter plasmid pACYC184 (73) in preparations made from the different
202 strain derivatives.

203 The results, shown in Figure 2, indicate that (i) in MDS42, both *topA*
204 mutations tested confer increased supercoiling (compare lanes 3-6 with lanes
205 1-2); (ii) *rpoB*35* does not alter supercoiling, in both the *topA*$^+$ (compare within
206 lane pairs 1 and 2, or 8 and 9) and *topA* derivatives (compare within lane pairs

207 3 and 4, or 5 and 6); and (iii) supercoiling levels are not different between the
208 strain backgrounds of MG1655 and MDS42 for both *rpoB*$^+$ (compare lanes 1
209 and 8) and the *rpoB*35* mutant (compare lanes 2 and 9). We conclude that
210 when lethality conferred by loss of Topo I is suppressed by either genome-size
211 reduction in MDS42 or *rpoB*35*, or by both perturbations together, there is
212 no concomitant reduction in the hypernegative supercoiling status of DNA in
213 these mutants.

214 ***topA* lethality in MG1655 is not rescued by ectopic expression of the R-**
215 **loop helicase UvsW.** Ectopic expression of the phage T4-encoded R-loop
216 helicase UvsW (74) has previously been shown to rescue lethality associated
217 with increased R-loop prevalence in several different *E. coli* mutants. The
218 latter include strains with combined deficiency of RNases HI and HII (69), or
219 of RNase HI and RecG (75), as also those with deletions of genes *rho* or *nusG*
220 involved in factor-dependent transcription termination (69).

221 Since Topo I deficiency phenotypes are also associated with increased
222 occurrence of intracellular R-loops and are partially suppressed by RNase HI
223 overexpression (18, 21–23, 26–28), we employed the blue-white assays to
224 examine whether UvsW expression (from a P_{tac}-UvsW chromosomal construct,
225 induced with IPTG) could rescue MG1655 *topA* lethality; an MG1655 Δ*rho*
226 derivative (whose lethality is known to be rescued by UvsW) was chosen as
227 control. The results indicate that UvsW expression does not confer viability to
228 the MG1655 *topA* derivative, whereas it could do so to the Δ*rho* mutant (Supp.
229 Fig. S3B). UvsW expression was associated with impaired growth of the *topA*$^+$
230 blue colonies; this growth impairment was exemplified both by a marked
231 decrease in plating efficiency and by occurrence of blue haloes around the
232 colonies, suggestive of cell lysis. That UvsW expression is toxic to wild-type *E.*
233 *coli* has been reported earlier (69).

234 **Rescue of Δ*dnaA* lethality by Topo I deficiency.** As mentioned above, Topo
235 I deficiency was earlier shown by a biochemical assay to confer cSDR, but
236 whether it can rescue lethality associated with loss of DnaA function (that is,
237 the genetic assay for cSDR) has not been determined. We adapted the blue-
238 white assay to test whether any of the *topA* mutations can rescue lethality

239 associated with loss of DnaA function, by constructing a Tp^R *lacZ*$^+$ shelter
240 plasmid that carried both *topA*$^+$ and *dnaA*$^+$. Three different *dnaA* alleles were
241 used in these experiments: Δ*dnaA*::Kan (70), which is a Keio-style insertion-
242 deletion that has removed all but the first codon and the last six codons of
243 the 468-codon-long *dnaA* ORF; its FRT derivative, Δ*dnaA*::FRT (70); and
244 *dnaA177* (76), whose DNA sequence determination revealed that it carries
245 both a missense mutation in codon 267 (resulting in Thr-to-Ilv substitution)
246 and an amber nonsense mutation in codon 450. The strains also carried Δ*tus*
247 and *rpoB***35* mutations, which facilitate cSDR-directed chromosome
248 duplication by overcoming the problems posed, respectively, by the *Ter* sites
249 and by excessive head-on transcription-replication conflicts (52, 70, 77, 78).

250 Of the six *topA* mutations tested that had been shown above to be lethal
251 in MG1655, one (*topA*-Ins480::FRT) was able to rescue lethality of Δ*dnaA*::FRT
252 and of *dnaA177* at 30° on both minimal and LB media (Fig. 3A-B and Supp.
253 Fig. S4A), while the others yielded no viable white colonies (Fig. 3A). Even with
254 *topA*-Ins480::FRT, there was no rescue imposed by DnaA deficiency at 37° or
255 42° (Fig. 3B, see also row 5 in each of the panels of Supp. Fig. S5), nor were
256 viable colonies recovered with the Δ*dnaA*::Kan allele (Fig. 3A). On the other
257 hand, Δ*dnaA*::Kan lethality is rescued by other cSDR-provoking mutations
258 such as *rnhA* or *dam* (data not shown).

259 Two distinct and interesting interpretations are suggested from these
260 data: (i) that unlike the other five *topA* alleles, *topA*-Ins480::FRT might possess
261 a low level of DNA relaxation activity (since it encodes a full-length polypeptide
262 with just a 27-amino acid linker inserted between residues 480 and 481 of
263 Topo I) which is not sufficient for viability *per se* in MG1655 but nonetheless
264 is necessary for viability in the derivatives whose sole source of chromosome
265 duplication is cSDR; and (ii) that expression of the essential *dnaN* gene
266 immediately downstream of, and in the same operon as, *dnaA* is achieved
267 from a fortuitous outward reading promoter in the Kan^R element of the
268 Δ*dnaA*::Kan allele, but that this promoter is rendered inactive under TopoI-
269 deficient conditions.

270 Notwithstanding these unusual features, our data clearly establish that

271 cSDR in a Topo I-deficient derivative can act to rescue the lethality associated
272 with total absence of DnaA in the cells. This viability is contingent on absence
273 of the Tus protein (Supp. Fig. S4B). On the other hand, the DinG helicase,
274 which has been shown to be needed for Δ*dnaA* viability of RecG- or Dam-
275 deficient cells (70), was not so required in the Topo I-deficient strain, nor did
276 its absence impede viability of the *topA* mutant in the *dnaA*$^+$ derivative (Supp.
277 Fig. S4C).

278 **Copy number analysis of different chromosomal regions in *topA* mutants.**
279 In an exponentially growing population of bacterial cells, DnaA-initiated
280 replication imposes a bidirectional gradient of copy number for different
281 regions of the circular chromosome, with the peak near *oriC* and trough in the
282 terminus region (53). If a *dnaA*$^+$ strain also suffers a perturbation that
283 activates cSDR (such as deficiency of RNase HI, RecG, Dam, or multiple DNA
284 exonucleases), the DNA copy number pattern is characterized by
285 superposition of a "mid-terminus peak" on the bidirectional gradient
286 described above (52, 70, 77–82). We have earlier proposed that the mid-
287 terminus peak represents a population aggregate of replication forks
288 progressing from stochastically firing cSDR origins that are widely distributed
289 across the genome (53, 70), although other groups have suggested that it
290 represents a discrete origin of replication (52, 77–79), or occurrence of over-
291 replication when oppositely directed forks converge at the terminus (80, 81).

292 Drolet and coworkers have shown earlier that Topo I-deficient mutants
293 exhibit the mid-terminus peak (19), but their strains also carried additional
294 genetic changes such as a *gyrB* (Ts) mutation and amplification of the genes
295 encoding subunits of topoisomerase IV. For our DNA copy number analysis
296 studies, we used *dnaA*$^+$ strains of the MDS42 background without or with
297 *rpoB*35* and additionally with the *topA*-Ins480::FRT mutation (that is, the
298 allele associated with rescue of Δ*dnaA* inviability).

299 The whole genome sequence reads obtained from each of the strains
300 were aligned to the MDS42 reference sequence, and normalized read counts
301 for the different chromosomal regions were determined. No suppressor
302 mutation in any of the candidate genes was identified in the *topA* mutants,

303 while presence of the *topA* mutation itself and of the CAC-to-CAA codon
304 change (His-to-Gln substitution) associated with the *rpoB*35* allele (60) was
305 confirmed in each of the relevant strains.

306 The parental (*topA*$^+$ *rpoB*$^+$) strain exhibited the expected bidirectional
307 copy number gradient from *oriC* to *Ter* (Fig. 4, panel i), which was also largely
308 preserved in its *rpoB*35* derivative (Fig. 4, panel ii). The *topA* mutant
309 derivatives of both these strains showed distinct mid-terminus peaks
310 superimposed on the *oriC*-to-*Ter* gradient (Fig. 4, panels iii and iv,
311 respectively).

312 These results therefore confirm that a *topA* mutation capable of
313 conferring Δ*dnaA* viability is associated with a mid-terminus peak of DNA copy
314 number in *dnaA*$^+$ derivatives.

315 **Mutual suppression between lethal mutations: loss of DnaA suppresses**
316 ***topA*-*rnhA* synthetic lethality.** Deficiency of either Topo I or RNase HI is
317 associated with cSDR, and Stockum et al. (13) as well as Drolet and coworkers
318 (26, 29) have earlier reported lethality or aggravated sickness in the double-
319 deficient strains. We too found in this study that introduction of the *rnhA*
320 mutation into otherwise viable *topA* derivatives (that is, in the MG1655-
321 derived strain with *rpoB*35* and Δ*tus* mutations) confers synthetic lethality;
322 the two *topA* alleles tested were the FRT derivatives of *topA*-Ins480 and Δ*topA*
323 (Fig. 5, compare panels i-ii for former, and iv-v for latter). The lethalities were
324 rescued in presence of Δ*dnaA* (Fig. 5, panels iii and vi, respectively), indicating
325 that two otherwise lethal mutant combinations (*topA rnhA* and *dnaA*) could
326 mutually suppress one another. Robust viability of the triple mutants was
327 observed on both rich and defined media at 30° and 37°, less so at 42° (Supp.
328 Fig. S5).

329 We performed PCR experiments to confirm that the chromosomal *topA*
330 locus in each of the viable triple mutant *topA rnhA dnaA* derivatives was
331 indeed disrupted (and had not, for example, become *topA*$^+$ by gene conversion
332 from the wild-type allele on the shelter plasmid). Two primer pairs were used
333 simultaneously to distinguish between the *topA*$^+$, Δ*topA*::FRT, and *topA*-

334 Ins480::FRT alleles, that yielded amplicons of 500, 328, and 581 bp,
335 respectively (Supp. Fig. S6A-B). The results established that the signatures
336 for the *topA*-Ins480 and Δ*topA* mutations were present, and that for *topA*$^+$ was
337 absent, in the triple mutant strains (Supp. Fig. S6B, lanes 5 and 7,
338 respectively).

339 As discussed below, these results suggest that it is excessive
340 chromosomal replication which kills cells doubly defective for Topo I and
341 RNase HI.

342 **Discussion**

343 The enzymes Topo I and DNA gyrase act to maintain the homeostatic
344 balance of DNA negative supercoiling in *E. coli*. Topo I relaxes negative
345 supercoils, especially those occurring behind RNAP during transcription
346 elongation, and thus prevents the nascent transcript from re-annealing with
347 the template DNA strand to form R-loops.

348 In this study, we have confirmed that Topo I-deficient *E. coli* mutants
349 are inviable, and furthermore have identified two novel means by which the
350 lethality can be independently and additively suppressed: (i) by deletion of the
351 non-essential 14% of the genome comprising prophages and transposable
352 elements, as in the strain MDS42; and (ii) by the *rpoB*35* mutation encoding
353 an altered RNAP which has earlier been variously described (not mutually
354 exclusive) to mimic the transcriptional effects of ppGpp (60), to reduce RNAP
355 backtracking (40), and to mitigate the effects of transcription-replication
356 conflicts by destabilizing the TEC (40, 52, 62, 63, 65). Neither of the
357 suppressors acts by reversing hypernegative supercoiling in the *topA*
358 mutants. We have also shown that Topo I deficiency, in the presence of
359 additional *rpoB*35* and Δ*tus* mutations, can rescue Δ*dnaA* lethality, thereby
360 providing genetic confirmation for occurrence of cSDR in the Topo I-deficient
361 derivatives.

362 ***rpoB*35* and RNAP backtracking.** As mentioned above, several workers have
363 provided evidence that the *rpoB*35*-encoded substitution in RNAP destabilizes
364 the TEC in vitro (40, 62) and protects against transcription-replication

365 conflicts in vivo (65), including during cSDR (52, 70, 77, 78). Trautinger and
366 Lloyd (61) have reported that *rpoB*35* suppresses the Ts phenotype of *greA*
367 *greB* double mutants and the UV-sensitivity of an *mfd* mutant, which they
368 interpret as evidence that it may function by preventing backtracking, thus
369 facilitating dissociation of stalled TECs. Likewise, *rpoB*35* also suppresses *rep*
370 *uvrD* lethality, which has been ascribed to direct reduction of replicative
371 barriers posed by TECs under these conditions (63).

372 On the other hand, there is one report from the Nudler group that
373 RpoB*35-substituted RNAP exhibits increased backtracking in vitro in
374 presence of UvrD (64). This property of RpoB*35-RNAP appears to be strictly
375 UvrD-dependent, and the same group has shown in other studies (40) that
376 relative to wild-type RNAP, the RpoB*35 enzyme is resistant to pausing and
377 backtracking.

378 It is therefore reasonable to conclude that the RpoB*35 enzyme is in
379 general more resistant than wild-type RNAP to arrest and backtracking during
380 transcription elongation, except perhaps in the specific context when a high
381 concentration of UvrD dimers occurs following DNA damage. Our finding in
382 this study, that the suppression of *topA* lethality by *rpoB*35* is UvrD-
383 independent (Supp. Fig. S3A), is noteworthy in this context.

384 **Mechanism of lethality in Topo I-deficient strains.** The fact that *rpoB*35*
385 restores growth to MG1655 in absence of Topo I without affecting the
386 hypernegative supercoiling status of the mutants suggests that it is the
387 downstream consequences of increased negative supercoiling, namely RNAP
388 backtracking and impairment of TEC progression leading to transcription-
389 replication conflicts, which are responsible for *topA* lethality. Pathological R-
390 loop formation is also expected to be an important feature at the arrested
391 TECs, but whether it precedes or follows RNAP backtracking remains to be
392 determined. In the *topA* mutant, *rpoB*35* would also relieve the sickness
393 during cSDR engendered by transcription-replication conflicts especially at
394 the *rrn* operons.

395 To explain *topA* viability in MDS42, we propose that the regions of the
396 genome that are deleted in this strain (comprising prophages and
397 transposable elements) are preferentially enriched for sites of R-loop
398 formation, TEC arrest and transcription-replication conflict. Loss of the
399 proteins Rho or NusG, that are involved in factor-dependent transcription
400 termination and reportedly in R-loop avoidance (31, 69, 83-85), is also better
401 tolerated in MDS42 than in MG1655, and especially so in presence of *rpoB*35*
402 (65, 69, 86).

403 Finally, why does ectopic expression of the R-loop helicase UvsW not
404 rescue *topA* lethality, although it can rescue the lethalities associated with
405 loss of RNase H enzymes, RecG, Rho or NusG (69, 75)? One possibility is that
406 R-loop formation in Topo I-deficient strains is a consequence, and not cause,
407 of RNAP backtracking and arrest, so that R-loop removal per se would not
408 mitigate the primary problem. An alternative possibility is that Topo I itself is
409 required to relax the negative supercoils arising from UvsW's helicase action
410 on R-loops, and hence that UvsW is unable to act efficiently to unwind R-
411 loops specifically in the *topA* mutants. The fact that RNase HI overexpression
412 can suppress *topA* sickness phenotypes (26, 27) lends support to the second
413 model.

414 **Topo I deficiency and cSDR.** Drolet and coworkers had provided biochemical
415 evidence for cSDR in Topo I-deficient cultures (28), which is presumably
416 initiated from R-loops in these cells; our data establish that such cSDR is
417 sufficient to sustain viability in absence of DnaA, in derivatives carrying Δ*tus*
418 and *rpoB*35* mutations. The latter two mutations are expected to facilitate the
419 completion of replication of the circular chromosome by forks initiated from
420 site(s) other than *oriC* (52, 70, 77, 78). Our data also support the earlier
421 suggestion (70) that incubation at 30° is more permissive than that at 37° or
422 42° for rescue by cSDR of Δ*dnaA* lethality.

423 Of the six different *topA* mutations that were inviable in MG1655-
424 derived strains, it was only the *topA*-Ins480::FRT allele that could confer
425 viability to the Δ*dnaA* derivatives. As explained above, this mutation generates
426 a modified version of Topo I in which a 27 amino acid-linker is inserted

427 between residues 480 and 481 of the polypeptide. From the Topo I monomer
428 crystal structure (87, 88), it is expected that the linker is situated at or near
429 the junction between residues that comprise domain D2 and those that
430 comprise domain D4; it is therefore possible that the linker may allow for (the
431 albeit inefficient) folding of the polypeptide to yield a correct tertiary structure.
432 The residual Topo I activity of this protein might be needed for proper
433 chromosome segregation after cSDR in the Δ*dnaA* mutants (20).

434 ***oriC*-initiated replication contributes to *topA-rnhA* synthetic lethality.**
435 We have shown that although the Δ*topA* and Δ*rnhA* combination is
436 synthetically lethal, the Δ*topA* Δ*rnhA* Δ*dnaA* mutant is viable. Thus, *oriC*-
437 initiated replication is a contributor to *topA rnhA* toxicity, which suggests that
438 it is excessive replication (sum of that from *oriC* and cSDR, the latter
439 contributed additively by both *rnhA* and *topA*) which confers toxicity. These
440 results are in agreement with those from Drolet and coworkers (20, 29), who
441 had earlier reported that mutations affecting either replication from *oriC* or
442 replication restart functions can alleviate the sickness of cells deficient for
443 both Topo I and RNase HI activities.

444 **Materials and Methods**

445 **Growth media, bacterial strains and plasmids**. The rich and defined growth
446 media were, respectively, LB and minimal A with 0.2% glucose (89) and,
447 unless otherwise indicated, the growth temperature was 37°.
448 Supplementation with Xgal and with antibiotics ampicillin, kanamycin (Kan),
449 tetracycline (Tet), chloramphenicol (Cm), and trimethoprim (Tp) were at the
450 concentrations described earlier (90). Isopropyl-β-D-thiogalactoside (IPTG)
451 was added at the indicated concentrations. *E. coli* strains used are listed in
452 Table S1, in the supplemental material.

453 Plasmids described earlier include pMU575 (Tp^R, single-copy-number
454 vector with *lacZ*$^+$) (68); pACYC184 (Tet^R Cm^R, p15A replicon) (73); pHYD2388
455 (70) and pHYD2411 (69) (Tp^R, pMU575 derivatives with, respectively, *dnaA*$^+$
456 and *rho*$^+$); and pKD13, pKD46 and pCP20 described by Datsenko and Wanner
457 (66) for recombineering experiments and Flp-recombinase catalyzed excision
458 between a pair of FRT sites. The construction of two derivatives of plasmid

459 pMU575 is described in the supplemental material: pHYD2382, carrying
460 *topA*$^+$, and pHYD2390, carrying *topA*$^+$ *dnaA*$^+$.
461 **Blue-white screening assays.** To determine lethality or viability of strains
462 with chromosomal *topA* or *dnaA* mutations, derivatives carrying the shelter
463 plasmids pHYD2382 (*topA*$^+$) or pHYD2390 (*topA*$^+$ *dnaA*$^+$) were grown overnight
464 in Tp-supplemented medium, subcultured into medium without Tp for growth
465 to mid-exponential phase, and plated at suitable dilutions on Xgal plates
466 without Tp. The percentage of white colonies to total was determined
467 (minimum of 500 colonies counted), and representative images were captured.
468 **Plasmid supercoiling assays.** Strains carrying plasmid pACYC184 were
469 grown in LB to mid-exponential phase, and plasmid preparations were made
470 with the aid of a commercial kit. Plasmid supercoiling status in each of the
471 preparations was determined essentially as described (72), following
472 electrophoresis on 1% agarose gel with 5 μg/ml chloroquine at 3 V/cm for 17
473 hr.
474 **Copy number analysis by deep sequencing.** Copy number determinations
475 of the various genomic regions were performed essentially as described (70).
476 Genomic DNA was extracted by the phenol-chloroform method from cultures
477 grown in LB to mid-exponential phase, and single-end deep sequencing was
478 performed on Illumina platforms to achieve around 100-fold coverage for each
479 preparation. Sequence reads were aligned to the MDS42 reference genome
480 (Accession number NC_020518.1), and copy numbers were then determined
481 by a moving-average method after normalization of the base read count for
482 each region to the aggregate of aligned base read counts for that culture.

483 **Other methods.** Procedures were as described for P1 transduction (91) and
484 for recombinant DNA manipulations, PCR, and transformation (92). Different
485 chromosomal *topA* mutations were generated by recombineering (66) as
486 described in the supplemental material. For microscopy experiments, cells
487 from cultures grown in LB to mid-exponential phase were immobilized on 1%
488 agarose pads and visualized by differential interference contrast imaging with
489 the aid of a Zeiss Axio Imager Z2 microscope.

490 **Data availability.** Genome sequence data from this work have been

491 submitted under Accession number PRJNA670792 and are available for
492 public access at https://www.ncbi.nlm.nih.gov/Traces/study/?acc=PRJNA670792 .

493 **Supplemental material**

494 Supplemental material is provided as a PDF file "Supplemental File 1".

495 **Acknowledgements**

496 We thank Jillella Mallikarjun for sequencing the *dnaA177* allele; Aswin
497 Seshasayee and T V Reshma for help with deep sequencing; V Balaji for
498 assistance with microscopy; and the COE team members for advice and
499 discussions.

500 This work was supported by Government of India funds from (i) DBT
501 Centre of Excellence (COE) project for Microbial Biology – Phase 2, (ii) SERB
502 project CRG/2018/000348, and (iii) DBT project
503 BT/PR34340/BRB/10/1815/2019. JG was recipient of the J C Bose
504 fellowship and INSA Senior Scientist award.

505 We declare that there are no conflicts of interest.

506 **References**

507 1. Vos SM, Tretter EM, Schmidt BH, Berger JM. 2011. All tangled up: how
508 cells direct, manage and exploit topoisomerase function. Nat Rev Mol
509 Cell Biol 12:827–841.
510 2. Chen SH, Chan NL, Hsieh TS. 2013. New mechanistic and functional
511 insights into DNA topoisomerases. Annu Rev Biochem 82:139–170.
512 3. Bush NG, Evans-Roberts K, Maxwell A. 2015. DNA topoisomerases.
513 EcoSal Plus doi:10.1128/ecosalplus.ESP-0010-2014.
514 4. Brochu J, Breton E V, Drolet M. 2020. Supercoiling, R-loops, Replication
515 and the Functions of Bacterial Type 1A Topoisomerases. Genes 11:pli-
516 E249.
517 5. Liu LF, Wang JC. 1987. Supercoiling of the DNA template during
518 transcription. Proc Natl Acad Sci U S A 84:7024–7027.
519 6. Dorman CJ. 2019. DNA supercoiling and transcription in bacteria: a
520 two-way street. BMC Mol cell Biol 20:26.
521 7. Sternglanz R, DiNardo S, Voelkel KA, Nishimura Y, Hirota Y, Becherer

522 K, Zumstein L, Wang JC. 1981. Mutations in the gene coding for
523 *Escherichia coli* DNA topoisomerase I affect transcription and
524 transposition. Proc Natl Acad Sci U S A 78:2747–2751.
525 8. Richardson SM, Higgins CF, Lilley DM. 1984. The genetic control of DNA
526 supercoiling in *Salmonella typhimurium*. EMBO J 3:1745–1752.
527 9. Ni Bhriain N, Dorman CJ. 1993. Isolation and characterization of a *topA*
528 mutant of *Shigella flexneri*. Mol Microbiol 7:351–358.
529 10. McNairn E, Ni Bhriain N, Dorman CJ. 1995. Overexpression of the
530 *Shigella flexneri* genes coding for DNA topoisomerase IV compensates for
531 loss of DNA topoisomerase I: effect on virulence gene expression. Mol
532 Microbiol 15:507–517.
533 11. Reddy M, Gowrishankar J. 1997. Identification and characterization of
534 *ssb* and *uup* mutants with increased frequency of precise excision of
535 transposon Tn*10* derivatives: nucleotide sequence of *uup* in *Escherichia*
536 *coli*. J Bacteriol 179:2892–2899.
537 12. Stupina VA, Wang JC. 2005. Viability of *Escherichia coli topA* mutants
538 lacking DNA topoisomerase I. J Biol Chem 280:355–360.
539 13. Stockum A, Lloyd RG, Rudolph CJ. 2012. On the viability of *Escherichia*
540 *coli* cells lacking DNA topoisomerase I. BMC Microbiol 12:26.
541 14. DiNardo S, Voelkel KA, Sternglanz R, Reynolds AE, Wright A. 1982.
542 *Escherichia coli* DNA topoisomerase I mutants have compensatory
543 mutations in DNA gyrase genes. Cell 31:43–51.
544 15. Pruss GJ, Manes SH, Drlica K. 1982. *Escherichia coli* DNA
545 topoisomerase I mutants: increased supercoiling is corrected by
546 mutations near gyrase genes. Cell 31:35–42.
547 16. Raji A, Zabel DJ, Laufer CS, Depew RE. 1985. Genetic analysis of
548 mutations that compensate for loss of *Escherichia coli* DNA
549 topoisomerase I. J Bacteriol 162:1173–1179.
550 17. Zhu Q, Pongpech P, DiGate RJ. 2001. Type I topoisomerase activity is
551 required for proper chromosomal segregation in *Escherichia coli*. Proc
552 Natl Acad Sci U S A 98:9766–9771.
553 18. Broccoli S, Phoenix P, Drolet M. 2000. Isolation of the *topB* gene
554 encoding DNA topoisomerase III as a multicopy suppressor of *topA* null

555 mutations in *Escherichia coli*. Mol Microbiol 35:58–68.
556 19. Brochu J, Vlachos-Breton E, Sutherland S, Martel M, Drolet M. 2018.
557 Topoisomerases I and III inhibit R-loop formation to prevent unregulated
558 replication in the chromosomal Ter region of *Escherichia coli*. PLoS Genet
559 14:e1007668.
560 20. Usongo V, Drolet M. 2014. Roles of type 1A topoisomerases in genome
561 maintenance in *Escherichia coli*. PLoS Genet 10:e1004543.
562 21. Drolet M, Bi X, Liu LF. 1994. Hypernegative supercoiling of the DNA
563 template during transcription elongation *in vitro*. J Biol Chem 269:2068–
564 2074.
565 22. Masse E, Phoenix P, Drolet M. 1997. DNA topoisomerases regulate R-
566 loop formation during transcription of the *rrnB* operon in *Escherichia*
567 *coli*. J Biol Chem 272:12816–12823.
568 23. Masse E, Drolet M. 1999. *Escherichia coli* DNA topoisomerase I inhibits
569 R-loop formation by relaxing transcription-induced negative
570 supercoiling. J Biol Chem 274:16659–16664.
571 24. Drolet M. 2006. Growth inhibition mediated by excess negative
572 supercoiling: the interplay between transcription elongation, R-loop
573 formation and DNA topology. Mol Microbiol 59:723–730.
574 25. Belotserkovskii BP, Tornaletti S, D'Souza AD, Hanawalt PC. 2018. R-
575 loop generation during transcription: Formation, processing and cellular
576 outcomes. DNA Repair (Amst) 71:69–81.
577 26. Drolet M, Phoenix P, Menzel R, Masse E, Liu LF, Crouch RJ. 1995.
578 Overexpression of RNase H partially complements the growth defect of
579 an *Escherichia coli* delta *topA* mutant: R-loop formation is a major
580 problem in the absence of DNA topoisomerase I. Proc Natl Acad Sci U S
581 A 92:3526–3530.
582 27. Masse E, Drolet M. 1999. R-loop-dependent hypernegative supercoiling
583 in *Escherichia coli topA* mutants preferentially occurs at low
584 temperatures and correlates with growth inhibition. J Mol Biol 294:321–
585 332.
586 28. Martel M, Balleydier A, Sauriol A, Drolet M. 2015. Constitutive stable
587 DNA replication in *Escherichia coli* cells lacking type 1A topoisomerase

588 activity. DNA Repair (Amst) 35:37–47.
589 29. Usongo V, Martel M, Balleydier A, Drolet M. 2016. Mutations reducing
590 replication from R-loops suppress the defects of growth, chromosome
591 segregation and DNA supercoiling in cells lacking topoisomerase I and
592 RNase HI activity. DNA Repair (Amst) 40:1–17.
593 30. Hraiky C, Raymond MA, Drolet M. 2000. RNase H overproduction
594 corrects a defect at the level of transcription elongation during rRNA
595 synthesis in the absence of DNA topoisomerase I in *Escherichia coli*. J
596 Biol Chem 275:11257–11263.
597 31. Raghunathan N, Kapshikar RM, Leela JK, Mallikarjun J, Bouloc P,
598 Gowrishankar J. 2018. Genome-wide relationship between R-loop
599 formation and antisense transcription in *Escherichia coli*. Nucleic Acids
600 Res 46:3400–3411.
601 32. Gan W, Guan Z, Liu J, Gui T, Shen K, Manley JL, Li X. 2011. R-loop-
602 mediated genomic instability is caused by impairment of replication fork
603 progression. Genes Dev 25:2041–2056.
604 33. Gómez-González B, Aguilera A. 2019. Transcription-mediated
605 replication hindrance: A major driver of genome instability. Genes Dev.
606 33:1008–1026.
607 34. Garcia-Muse T, Aguilera A. 2019. R Loops: From Physiological to
608 Pathological Roles. Cell 179:604–618.
609 35. Ivanov IE, Wright A V, Cofsky JC, Aris KDP, Doudna JA, Bryant Z. 2020.
610 Cas9 interrogates DNA in discrete steps modulated by mismatches and
611 supercoiling. Proc Natl Acad Sci U S A 117:5853–5860.
612 36. El Hage A, French SL, Beyer AL, Tollervey D. 2010. Loss of
613 Topoisomerase I leads to R-loop-mediated transcriptional blocks during
614 ribosomal RNA synthesis. Genes Dev 24:1546–1558.
615 37. Tuduri S, Crabbe L, Conti C, Tourriere H, Holtgreve-Grez H, Jauch A,
616 Pantesco V, De Vos J, Thomas A, Theillet C, Pommier Y, Tazi J, Coquelle
617 A, Pasero P. 2009. Topoisomerase I suppresses genomic instability by
618 preventing interference between replication and transcription. Nat Cell
619 Biol 11:1315–1324.
620 38. Zhang T, Wallis M, Petrovic V, Challis J, Kalitsis P, Hudson DF. 2019.

621 Loss of TOP3B leads to increased R-loop formation and genome
622 instability. Open Biol 9:190222.
623 39. Boubakri H, de Septenville AL, Viguera E, Michel B. 2010. The helicases
624 DinG, Rep and UvrD cooperate to promote replication across
625 transcription units *in vivo*. EMBO J 29:145–157.
626 40. Dutta D, Shatalin K, Epshtein V, Gottesman ME, Nudler E. 2011.
627 Linking RNA polymerase backtracking to genome instability in *E. coli*.
628 Cell 146:533–543.
629 41. Lang KS, Hall AN, Merrikh CN, Ragheb M, Tabakh H, Pollock AJ,
630 Woodward JJ, Dreifus JE, Merrikh H. 2017. Replication-transcription
631 conflicts generate R-loops that orchestrate bacterial ctress survival and
632 pathogenesis. Cell 170:787-799.
633 42. Hamperl S, Bocek MJ, Saldivar JC, Swigut T, Cimprich KA. 2017.
634 Transcription-replication conflict orientation modulates R-loop levels
635 and activates distinct DNA damage responses. Cell 170:774-786.
636 43. Nudler E. 2012. RNA polymerase backtracking in gene regulation and
637 genome instability. Cell 149:1438–1445.
638 44. Lang KS, Merrikh H. 2018. The clash of macromolecular titans:
639 replication-transcription conflicts in bacteria. Annu Rev Microbiol
640 72:71–88.
641 45. Kuzminov A. 2018. When DNA topology turns deadly - RNA polymerases
642 dig in their R-loops to stand their ground: new positive and negative
643 (super)twists in the replication-transcription conflict. Trends Genet
644 34:111–120.
645 46. Zatreanu D, Han Z, Mitter R, Tumini E, Williams H, Gregersen L, Dirac-
646 Svejstrup AB, Roma S, Stewart A, Aguilera A, Svejstrup JQ. 2019.
647 Elongation factor TFIIS prevents transcription stress and R-loop
648 accumulation to maintain genome stability. Mol Cell 76:57-69.
649 47. Itoh T, Tomizawa J. 1980. Formation of an RNA primer for initiation of
650 replication of ColE1 DNA by ribonuclease H. Proc Natl Acad Sci U S A
651 77:2450–2454.
652 48. Kogoma T. 1997. Stable DNA replication: interplay between DNA
653 replication, homologous recombination, and transcription. Microbiol

654 Mol Biol Rev 61:212–238.
655 49. Drolet M, Brochu J. 2019. R-loop-dependent replication and genomic
656 instability in bacteria. DNA Repair (Amst) 84:102693.
657 50. Sinha AK, Possoz C, Leach DRF. 2020. The roles of bacterial DNA
658 double-strand break repair proteins in chromosomal DNA replication.
659 FEMS Microbiol Rev 44:351–368.
660 51. Stuckey R, Garcia-Rodriguez N, Aguilera A, Wellinger RE. 2015. Role for
661 RNA:DNA hybrids in origin-independent replication priming in a
662 eukaryotic system. Proc Natl Acad Sci U S A 112:5779–5784.
663 52. Rudolph CJ, Upton AL, Stockum A, Nieduszynski CA, Lloyd RG. 2013.
664 Avoiding chromosome pathology when replication forks collide. Nature
665 500:608–611.
666 53. Gowrishankar J. 2015. End of the beginning: elongation and
667 termination features of alternative modes of chromosomal replication
668 initiation in bacteria. PLoS Genet11:e1004909.
669 54. Tehranchi AK, Blankschien MD, Zhang Y, Halliday JA, Srivatsan A, Peng
670 J, Herman C, Wang JD. 2010. The transcription factor DksA prevents
671 conflicts between DNA replication and transcription machinery. Cell
672 141:595–605.
673 55. Zhang Y, Mooney RA, Grass JA, Sivaramakrishnan P, Herman C,
674 Landick R, Wang JD. 2014. DksA guards elongating RNA polymerase
675 against ribosome-stalling-induced arrest. Mol Cell 53:766–778.
676 56. Myka KK, Kusters K, Washburn R, Gottesman ME. 2019. DksA-RNA
677 polymerase interactions support new origin formation and DNA repair
678 in *Escherichia coli*. Mol Microbiol 111:1382–1397.
679 57. Ogawa T, Pickett GG, Kogoma T, Kornberg A. 1984. RNase H confers
680 specificity in the dnaA-dependent initiation of replication at the unique
681 origin of the *Escherichia coli* chromosome *in vivo* and *in vitro*. Proc Natl
682 Acad Sci U S A 81:1040–1044.
683 58. Kaguni JM, Kornberg A. 1984. Topoisomerase I confers specificity in
684 enzymatic replication of the *Escherichia coli* chromosomal origin. J Biol
685 Chem 259:8578–8583.
686 59. Posfai G, Plunkett 3rd G, Feher T, Frisch D, Keil GM, Umenhoffer K,

687 Kolisnychenko V, Stahl B, Sharma SS, de Arruda M, Burland V, Harcum
688 SW, Blattner FR. 2006. Emergent properties of reduced-genome
689 *Escherichia coli*. Science 312:1044–1046.
690 60. McGlynn P, Lloyd RG. 2000. Modulation of RNA polymerase by (p)ppGpp
691 reveals a RecG-dependent mechanism for replication fork progression.
692 Cell 101:35–45.
693 61. Trautinger BW, Lloyd RG. 2002. Modulation of DNA repair by mutations
694 flanking the DNA channel through RNA polymerase. EMBO J 21:6944–
695 6953.
696 62. Trautinger BW, Jaktaji RP, Rusakova E, Lloyd RG. 2005. RNA
697 polymerase modulators and DNA repair activities resolve conflicts
698 between DNA replication and transcription. Mol Cell 19:247–258.
699 63. Guy CP, Atkinson J, Gupta MK, Mahdi AA, Gwynn EJ, Rudolph CJ,
700 Moon PB, van Knippenberg IC, Cadman CJ, Dillingham MS, Lloyd RG,
701 McGlynn P. 2009. Rep provides a second motor at the replisome to
702 promote duplication of protein-bound DNA. Mol Cell 36:654–666.
703 64. Kamarthapu V, Epshtein V, Benjamin B, Proshkin S, Mironov A, Cashel
704 M, Nudler E. 2016. ppGpp couples transcription to DNA repair in *E. coli*.
705 Science 352:993–996.
706 65. Washburn RS, Gottesman ME. 2011. Transcription termination
707 maintains chromosome integrity. Proc Natl Acad Sci U S A 108:792–797.
708 66. Datsenko KA, Wanner BL. 2000. One-step inactivation of chromosomal
709 genes in *Escherichia coli* K-12 using PCR products. Proc Natl Acad Sci U
710 S A 97:6640–6645.
711 67. Baba T, Ara T, Hasegawa M, Takai Y, Okumura Y, Baba M, Datsenko
712 KA, Tomita M, Wanner BL, Mori H. 2006. Construction of *Escherichia*
713 *coli* K-12 in-frame, single-gene knockout mutants: the Keio collection.
714 Mol Syst Biol 2:2006 0008.
715 68. Andrews AE, Lawley B, Pittard AJ. 1991. Mutational analysis of
716 repression and activation of the *tyrP* gene in *Escherichia coli*. J Bacteriol
717 173:5068–5078.
718 69. Leela JK, Syeda AH, Anupama K, Gowrishankar J. 2013. Rho-dependent
719 transcription termination is essential to prevent excessive genome-wide

720 R-loops in *Escherichia coli*. Proc Natl Acad Sci U S A110:258–263.
721 70. Raghunathan N, Goswami S, Leela JK, Pandiyan A, Gowrishankar J.
722 2019. A new role for *Escherichia coli* Dam DNA methylase in prevention
723 of aberrant chromosomal replication. Nucleic Acids Res 47:5698–5711.
724 71. Ali N, Gowrishankar J. 2020. Cross-subunit catalysis and a new
725 phenomenon of recessive resurrection in *Escherichia coli* RNase E.
726 Nucleic Acids Res 48:847–861.
727 72. Dattananda CS, Rajkumari K, Gowrishankar J. 1991. Multiple
728 mechanisms contribute to osmotic inducibility of proU operon
729 expression in *Escherichia coli*: demonstration of two osmoresponsive
730 promoters and of a negative regulatory element within the first
731 structural gene. J Bacteriol 173:7481–7490.
732 73. Chang AC, Cohen SN. 1978. Construction and characterization of
733 amplifiable multicopy DNA cloning vehicles derived from the P15A
734 cryptic miniplasmid. J Bacteriol 134:1141–1156.
735 74. Dudas KC, Kreuzer KN. 2001. UvsW Protein regulates bacteriophage T4
736 origin-dependent replication by unwinding R-loops. Mol Cell Biol
737 21:2706–2715.
738 75. Carles-Kinch K, George JW, Kreuzer KN. 1997. Bacteriophage T4 UvsW
739 protein is a helicase involved in recombination, repair and the regulation
740 of DNA replication origins. EMBO J 16:4142–4151.
741 76. Wechsler JA, Gross JD. 1971. *Escherichia coli* mutants temperature-
742 sensitive for DNA synthesis. Mol Gen Genet 113:273–284.
743 77. Dimude JU, Stockum A, Midgley-Smith SL, Upton AL, Foster HA, Khan
744 A, Saunders NJ, Retkute R, Rudolph CJ. 2015. The consequences of
745 replicating in the wrong orientation: bacterial chromosome duplication
746 without an active replication origin. MBio 6:e01294-15.
747 78. Midgley-Smith SL, Dimude JU, Rudolph CJ. 2019. A role for 3'
748 exonucleases at the final stages of chromosome duplication in
749 *Escherichia coli*. Nucleic Acids Res 47:1847–1860.
750 79. Maduike NZ, Tehranchi AK, Wang JD, Kreuzer KN. 2014. Replication of
751 the *Escherichia coli* chromosome in RNase HI-deficient cells: multiple
752 initiation regions and fork dynamics. Mol Microbiol 91:39–56.

753 80. Wendel BM, Courcelle CT, Courcelle J. 2014. Completion of DNA
754 replication in *Escherichia coli*. Proc Natl Acad Sci U S A 111:16454–
755 16459.
756 81. Wendel BM, Cole JM, Courcelle CT, Courcelle J. 2018. SbcC-SbcD and
757 ExoI process convergent forks to complete chromosome replication. Proc
758 Natl Acad Sci U S A 115:349–354.
759 82. Azeroglu B, Mawer JS, Cockram CA, White MA, Hasan AM, Filatenkova
760 M, Leach DR. 2016. RecG Directs DNA Synthesis during Double-Strand
761 Break Repair. PLoS Genet 12:e1005799.
762 83. Harinarayanan R, Gowrishankar J. 2003. Host factor titration by
763 chromosomal R-loops as a mechanism for runaway plasmid replication
764 in transcription termination-defective mutants of *Escherichia coli*. J Mol
765 Biol 332:31–46.
766 84. Gowrishankar J, Harinarayanan R. 2004. Why is transcription coupled
767 to translation in bacteria? Mol Microbiol 54:598–603.
768 85. Gowrishankar J, Leela JK, Anupama K. 2013. R-loops in bacterial
769 transcription: their causes and consequences. Transcription 4:153–157.
770 86. Cardinale CJ, Washburn RS, Tadigotla VR, Brown LM, Gottesman ME
771 NE. 2008. Termination factor Rho and its cofactors NusA and NusG
772 silence foeign DNA in *E. coli*. Science 320:935–938.
773 87. Tan K, Zhou Q, Cheng B, Zhang Z, Joachimiak A, Tse-Dinh YC. 2015.
774 Structural basis for suppression of hypernegative DNA supercoiling by
775 *E. coli* topoisomerase I. Nucleic Acids Res 43:11031–11046.
776 88. Cao N, Tan K, Zuo X, Annamalai T, Tse-Dinh Y-C. 2020. Mechanistic
777 insights from structure of *Mycobacterium smegmatis* topoisomerase I
778 with ssDNA bound to both N- and C-terminal domains. Nucleic Acids
779 Res 48:4448–4462.
780 89. Miller JH. 1992. A Short Course in Bacterial Genetics: A Laboratory
781 Manual and Handbook for *Escherichia coli* and Related Bacteria. Cold
782 Spring Harb Lab Press NY.
783 90. Anupama K, Leela JK, Gowrishankar J. 2011. Two pathways for RNase
784 E action in *Escherichia coli* in vivo and bypass of its essentiality in
785 mutants defective for Rho-dependent transcription termination. Mol

786 Microbiol 82:1330-1348.
787 91. Gowrishankar J. 1985. Identification of osmoresponsive genes in
788 *Escherichia coli*: evidence for participation of potassium and proline
789 transport systems in osmoregulation. J Bacteriol 164:434–445.
790 92. Sambrook J, Russell D. 2001. Molecular Cloning: A Laboratory Manual.
791 3rd edn. Cold Spring Harb Lab Press NY.
792

793 **Legends to figures**

794 **Figure 1. (A)** Representations of *topA*$^+$ ORF delineating the encoded protein's
795 domains D1 to D9 (adapted from 87, 88), and of the constructed *topA* alleles
796 (three pairs) wherein the interrupted line segments represent deletions and
797 each inverted triangle represents the pair comprising either Kan^R insertion
798 (::Kan allele) or its FRT derivative (::FRT allele). **(B)** Blue-white screening assay
799 on LB medium, of MG1655 or MDS42 strain derivatives with the *topA*$^+$ shelter
800 plasmid pHYD2390 and the different *topA* alleles as indicated on the top of
801 each column; the *rpoB* allele status is indicated at left of each row. Examples
802 of white colonies are marked by the yellow arrows. From left to right, strains
803 used for the panels were pHYD2390 derivatives of: row 1, GJ13519, GJ15603,
804 GJ15604, GJ15688 and GJ16921; row 2, GJ16703, GJ16813, GJ16814,
805 GJ16815 and GJ16854; row 3, GJ12134, GJ16816, GJ16817, GJ16818 and
806 GJ18977; and row 4, GJ16819, GJ16820, GJ16821, GJ16822 and GJ17777.

807 **Figure 2.** Supercoiling status of reporter plasmid pACYC184 in *topA*$^+$ and
808 *topA* derivatives, as determined by chloroquine-agarose gel electrophoresis.
809 Genotypes at *topA* and *rpoB* loci are indicated on top of each lane; for *topA,* Δ
810 and 480 refer, respectively, to Δ*topA*::FRT and *topA*-Ins480::FRT. Strains for
811 different lanes were pACYC184 derivatives of: 1, GJ12134; 2, GJ16819; 3,
812 18976; 4, GJ18977; 5, GJ17776; 6, GJ17777; 8, GJ18601; and 9, GJ18910.
813 Lane 7, DNA size standards.

814 **Figure 3.** Suppression of Δ*dnaA* lethality by *topA*. **(A)** Blue-white screening
815 assay at 30° on glucose-minimal A with *topA*$^+$ *dnaA*$^+$ shelter plasmid
816 pHYD2390 in MG1655 Δ*dnaA* Δ*tus rpoB*35* derivatives carrying different *topA*
817 alleles; the nature of Δ*dnaA* allele (::Kan or ::FRT) and of *topA* allele are shown
818 on top of each panel. Examples of white colonies are marked by the yellow
819 arrows. Strains employed for the different panels were pHYD2390 derivatives
820 of: i, GJ17786; ii, GJ17790; iii, GJ18940; iv, GJ17787; v, GJ17791; vi,
821 GJ18941; vii, GJ17788; viii, GJ17792; and ix, GJ18942. **(B)** Serial dilution-
822 spotting on LB and glucose-minimal A (MM) at indicated temperatures of the
823 following derivatives of MG1655 Δ*tus rpoB*35*: Nil, *topA*$^+$ *dnaA*$^+$
824 (GJ17784/pHYD2390); *topA*, *topA*-Ins480::FRT *dnaA*$^+$ (GJ17784); and *topA*

825 *dnaA*, *topA*-Ins480::FRT Δ*dnaA*::FRT, that is, white colony from panel vi of
826 Figure 4A (GJ18941).
827 **Figure 4.** Copy number analysis by deep sequencing in *topA* mutant
828 derivatives of MDS42. In panels i to iv, relative copy numbers have been
829 plotted as semi-log graphs for overlapping 10-kb intervals across the genome
830 (relevant genotype of strain indicated on top of each panel); positions of *oriC,*
831 *TerA* and *TerC/B* are marked, and the gap at around 0.3 Mbp in each of the
832 plots corresponds to the *argF-lac* deletion present in the strains. Strains
833 displayed in the different panels are: i, GJ12134; ii, GJ16819; iii, GJ18977;
834 and iv, GJ17777.

835 **Figure 5.** Synthetic *topA rnhA* lethality, suppressed by Δ*dnaA*. Blue-white
836 screening assay at 30° on glucose-minimal A with *topA*$^+$ *dnaA*$^+$ shelter plasmid
837 pHYD2390 in MG1655 Δ*tus rpoB*35* derivatives carrying different alleles of
838 *topA*, *rnhA* and *dnaA* as indicated on top of each panel. Strains employed for
839 the different panels were pHYD2390 derivatives of: i, GJ17784; ii, GJ19609;
840 iii, GJ18951; iv, GJ17783; v, GJ19608; and vi, GJ18983.

Fig. 1

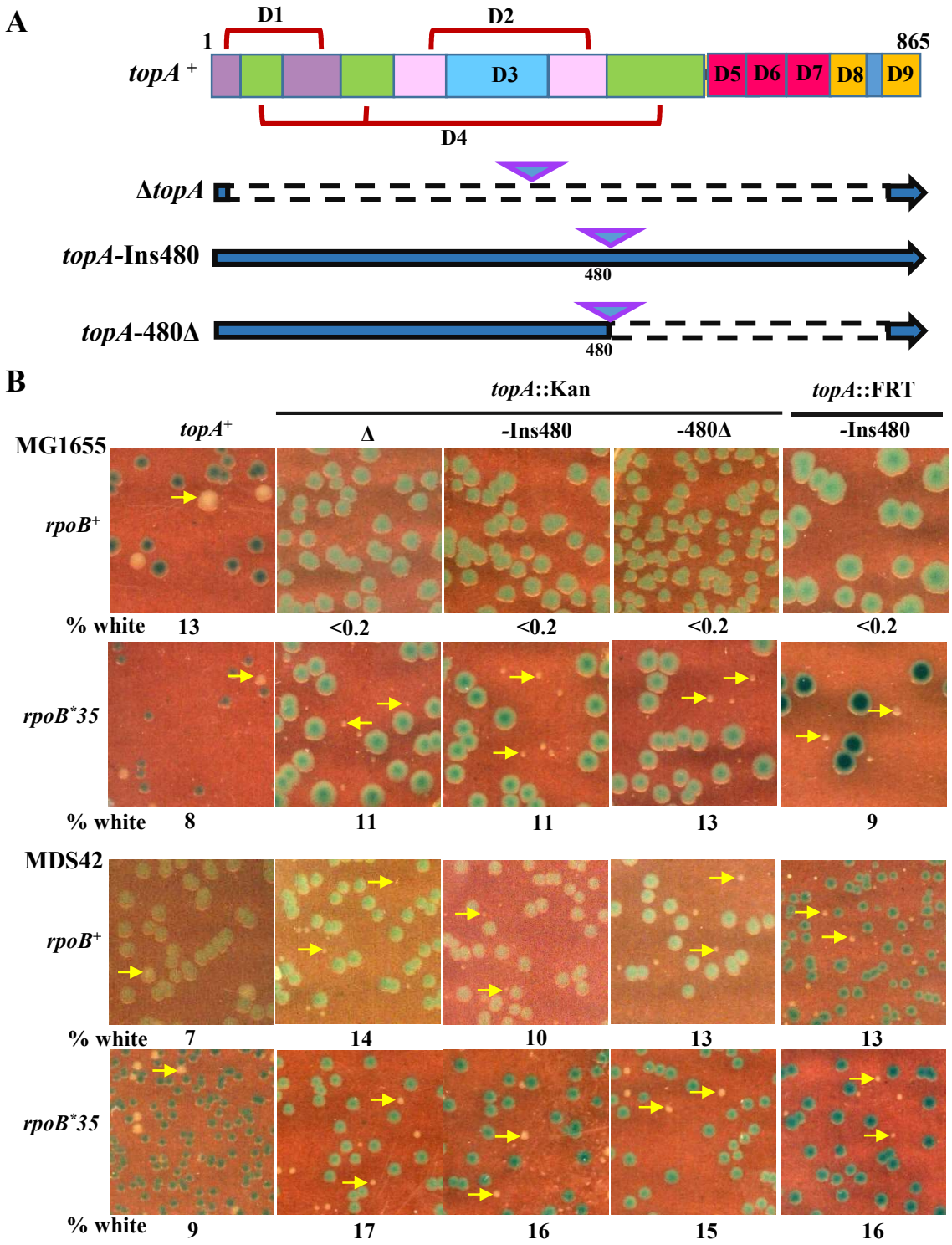

Figure 1. (A) Representations of *topA*$^+$ ORF delineating the encoded protein's domains D1 to D9 (adapted from 84, 85), and of the *topA* alleles (three pairs) constructed in this study wherein the interrupted line segments represent deletions and each inverted triangle represents the pair comprising either Kan^R insertion (::Kan allele) or its FRT derivative (::FRT allele). **(B)** Blue-white screening assay on LB medium, of MG1655 or MDS42 strain derivatives with the *topA*$^+$ shelter plasmid pHYD2390 and the different *topA* alleles as indicated on the top of each column; the *rpoB* allele status is indicated at left of each row. Examples of white colonies are marked by the yellow arrows. From left to right, strains used for the panels were pHYD2390 derivatives of: row 1, GJ13519, GJ15603, GJ15604, GJ15688 and GJ16921; row 2, GJ16703, GJ16813, GJ16814, GJ16815 and GJ16854; row 3, GJ12134, GJ16816, GJ16817, GJ16818 and GJ18977; and row 4, GJ16819, GJ16820, GJ16821, GJ16822 and GJ17777.

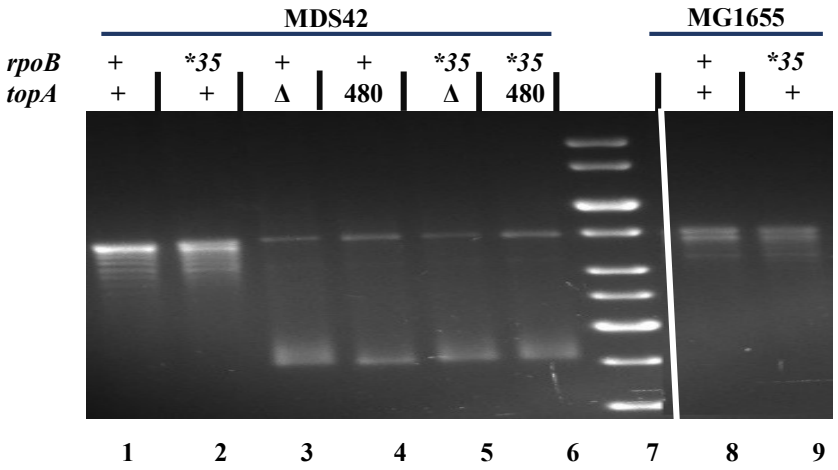

Figure 2. Supercoiling status of reporter plasmid pACYC184 in *topA*$^+$ and *topA* derivatives, as determined by chloroquine-agarose gel electrophoresis. Genotypes at *topA* and *rpoB* loci are indicated on top of each lane; for *topA,* Δ and 480 refer, respectively, to Δ*topA*::FRT and *topA*-Ins480::FRT. Strains for different lanes were pACYC184 derivatives of: 1, GJ12134; 2, GJ16819; 3, 18976; 4, GJ18977; 5, GJ17776; 6, GJ17777; 8, GJ18601; and 9, GJ18910. Lane 7, DNA size standards.

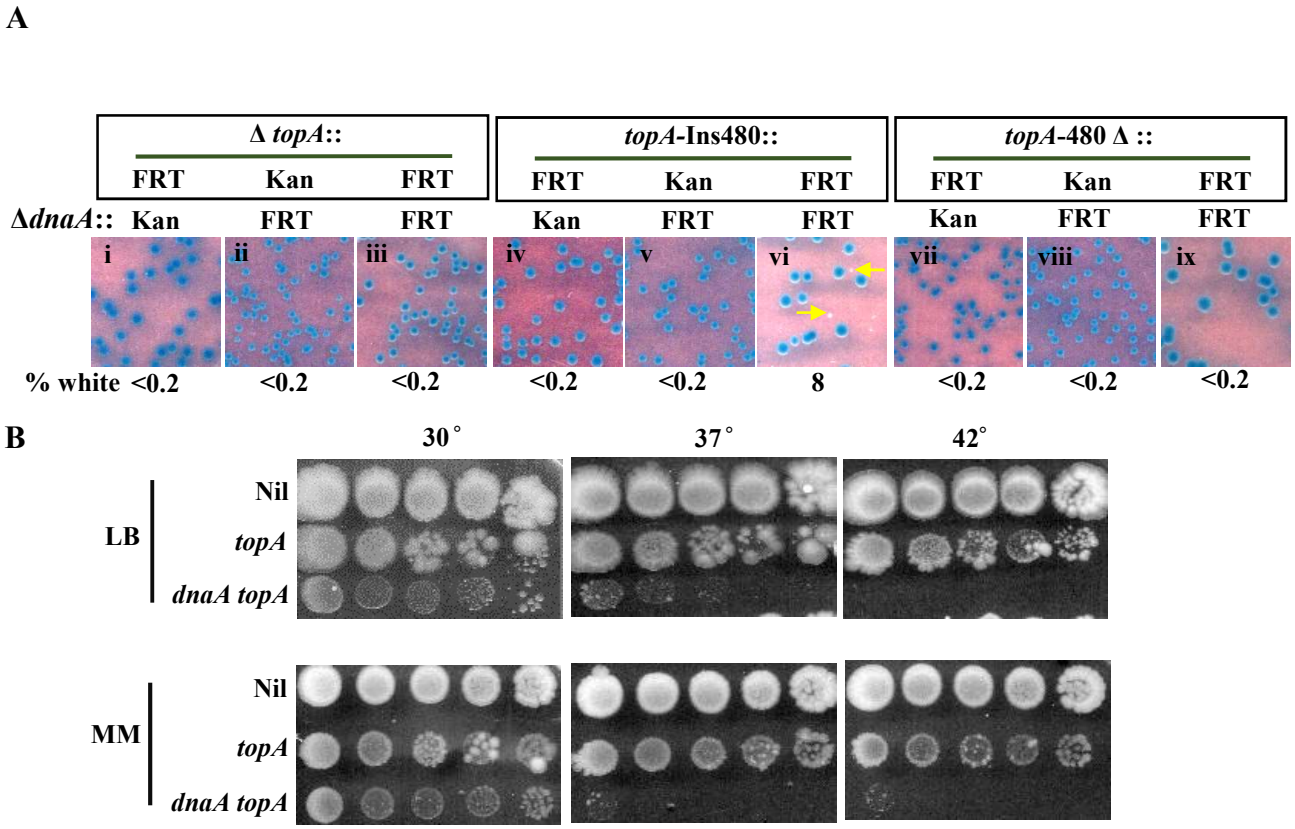

Figure 3. Suppression of Δ*dnaA* lethality by *topA*. **(A)** Blue-white screening assay at 30° on glucose-minimal A with *topA*$^+$ *dnaA*$^+$ shelter plasmid pHYD2390 in MG1655 Δ*dnaA* Δ*tus rpoB*35* derivatives carrying different *topA* alleles; the nature of Δ*dnaA* allele (::Kan or ::FRT) and of *topA* allele are shown on top of each panel. Examples of white colonies are marked by the yellow arrows. Strains employed for the different panels were pHYD2390 derivatives of: i, GJ17786; ii, GJ17790; iii, GJ18940; iv, GJ17787; v, GJ17791; vi, GJ18941; vii, GJ17788; viii, GJ17792; and ix, GJ18942. **(B)** Serial dilution-spotting on LB and glucose-minimal A (MM) at indicated temperatures of the following derivatives of MG1655 Δ*tus rpoB*35*: Nil, *topA*$^+$ *dnaA*$^+$ (GJ17784/pHYD2390); *topA*, *topA*-Ins480::FRT *dnaA*$^+$ (GJ17784); and *topA dnaA*, *topA*-Ins480::FRT Δ*dnaA*::FRT, that is, white colony from panel vi of Figure 4A (GJ18941).

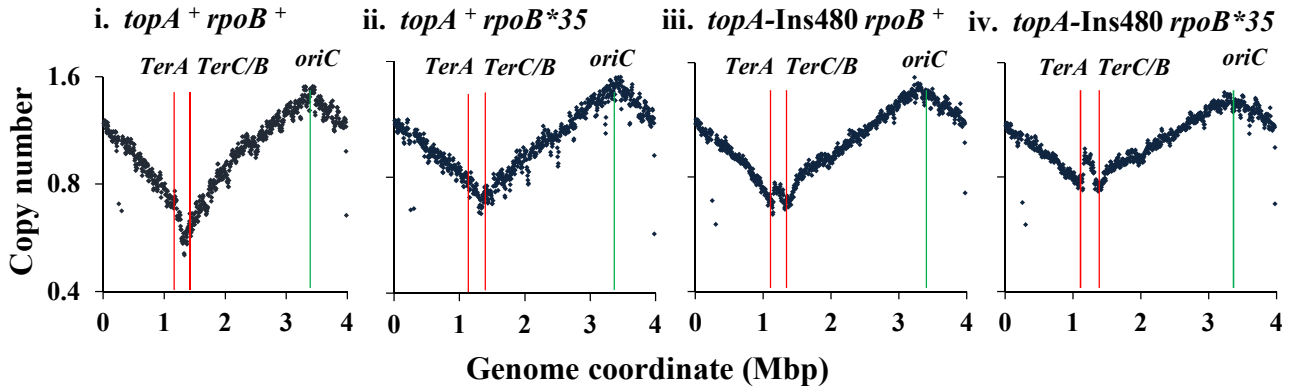

Figure 4. Copy number analysis by deep sequencing in *topA* mutant derivatives of MDS42. In panels i to iv, relative copy numbers have been plotted as semi-log graphs for overlapping 10-kb intervals across the genome (relevant genotypes of strain indicated on top of each panel); positions of *oriC, TerA* and *TerC/B* are marked, and the gap at around 0.3 Mbp in each of the plots corresponds to the *argF-lac* deletion present in the strains. Strains displayed in the different panels are: i, GJ12134; ii, GJ16819; iii, GJ18977; and iv, GJ17777.

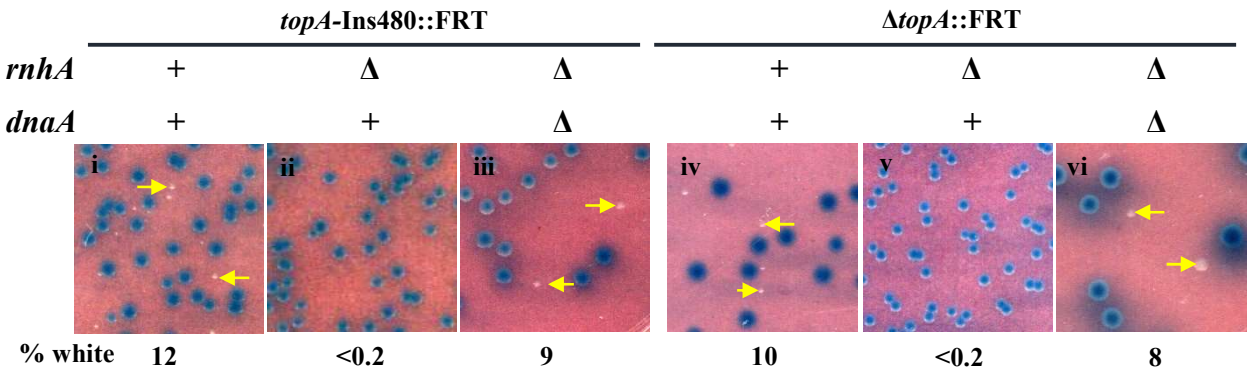

Figure 5. Synthetic *topA rnhA* lethality, suppressed by Δ*dnaA*. Blue-white screening assay at 30° on glucose-minimal A with *topA*⁺ *dnaA*⁺ shelter plasmid pHYD2390 in MG1655 Δ*tus rpoB*35* derivatives carrying different alleles of *topA*, *rnhA* and *dnaA* as indicated on top of each panel. Strains employed for the different panels were pHYD2390 derivatives of: i, GJ17784; ii, GJ19609; iii, GJ18951; iv, GJ17783; v, GJ19608; and vi, GJ18983.

Supplemental Material for

Topoisomerase I Essentiality, DnaA-independent Chromosomal Replication, and Transcription-Replication Conflict in *Escherichia coli*

J Krishna Leela[a], Nalini Raghunathan[a], and J Gowrishankar[a,b#]

[a]Laboratory of Bacterial Genetics, Centre for DNA Fingerprinting and Diagnostics, Hyderabad, India

[b]Indian Institute of Science Education and Research Mohali, SAS Nagar, India

Running Head: Topoisomerase I essentiality in *E. coli*

#Address correspondence to Dr J Gowrishankar (Orcid ID: 0000-0003-2483-9209), Tel: +91-172-2240266; Fax: +91-172-2240124; Email: shankar@iisermohali.ac.in

Keywords: DNA supercoiling, topoisomerase I, R-loops, constitutive stable DNA replication, transcription-replication conflict

Supplementary Methods

Construction of shelter plasmids pHYD2382 and pHYD2390. The pair of primers 5'-CCAAA*CTGCAG*TCGTGCTATAGCGCCTGT-3' and 5'-TTTGTT*AAGCTT*AACCTGACAGAATTAAAGG -3' (*PstI* and *HindIII* sites in them, respectively, italicized) were used with MG1655 genomic DNA to amplify the *topA*$^+$ gene by PCR, and the product was digested with *PstI* and *HindIII* before being cloned into the corresponding sites of plasmid vector pMU575, to generate the *topA*$^+$ shelter plasmid pHYD2382. The two primers are designated, respectively, as b1 and b2 in Supplementary Figure S7.

For constructing plasmid pHYD2390 (*topA*$^+$ *dnaA*$^+$ shelter plasmid), the DNA fragment present in plasmid pHYD2388 (1) carrying the *Salmonella enterica dnaA*$^+$ gene was sub-cloned *via* an intermediate plasmid vector into the *XbaI-KpnI* sites of plasmid pHYD2382.

Generation of *topA* mutations by recombineering. The Datsenko and Wanner method (2), with plasmids pKD13 and pKD46, was used for generating chromosomal *topA* mutations by recombineering in derivatives carrying the shelter plasmids pHYD2382 or pHYD2390. The primer pairs used for PCR with pKD13 template were: for Δ*topA*::Kan, 5'-TCAACGTGCGACGCATTCCTGGAAGAATCAAATTAGGTAAGGTGAATATGATTCCGGGGATCCGTCGACC-3' and 5'-TGTTTATAAAAACCTGACAGAATTAAAGGTTATTTTTTTCCTTCAACCCATGTAGGCTGGAGCTGCTTCG-3' (designated primer Y); for *topA*-Ins480::Kan, 5'-CCAGCACTTTACCAAGCCGCCAGCCCGTTTCAGTGAAGCAATTCCGGGGATCCGTCGACC-3' (designated primer X) and 5'-GACGACCGATACCGCGTTTTTCCAGCTCTTTAACCAGCGATGTAGGCTGGAGCTGCTTCG-3'; and for *topA*-480Δ, primers X and Y.

Given that the recombineering in these derivatives could have occurred on either the chromosome or the shelter plasmid, we employed simple genetic tests on several independent clones to classify them into the two categories. The three *topA*::FRT alleles on the chromosome were generated with the aid of plasmid pCP20, as described (2).

References

1. Raghunathan N, Goswami S, Leela JK, Pandiyan A, Gowrishankar J. 2019. A new role for *Escherichia coli* Dam DNA methylase in prevention of aberrant chromosomal replication. Nucleic Acids Res 47:5698–5711.

2. Datsenko KA, Wanner BL. 2000. One-step inactivation of chromosomal genes in *Escherichia coli* K-12 using PCR products. Proc Natl Acad Sci U S A 97:6640–6645.

3. Posfai G, Plunkett 3rd G, Feher T, Frisch D, Keil GM, Umenhoffer K, Kolisnychenko V, Stahl B, Sharma SS, de Arruda M, Burland V, Harcum SW, Blattner FR. 2006. Emergent properties of reduced-genome *Escherichia coli*. Science 312:1044–1046.

4. Leela JK, Syeda AH, Anupama K, Gowrishankar J. 2013. Rho-dependent transcription termination is essential to prevent excessive genome-wide R-loops in *Escherichia coli*. Proc Natl Acad Sci U S A 110:258–263.

5. Raghunathan N, Kapshikar RM, Leela JK, Mallikarjun J, Bouloc P, Gowrishankar J. 2018. Genome-wide relationship between R-loop formation and antisense transcription in *Escherichia coli*. Nucleic Acids Res 46:3400–3411.

6. Gowrishankar J. 1985. Identification of osmoresponsive genes in *Escherichia coli*: evidence for participation of potassium and proline transport systems in osmoregulation. J Bacteriol 164:434–445.

7. Wechsler JA, Gross JD. 1971. *Escherichia coli* mutants temperature-sensitive for DNA synthesis. Mol Gen Genet 113:273–284.

8. Baba T, Ara T, Hasegawa M, Takai Y, Okumura Y, Baba M, Datsenko KA, Tomita M, Wanner BL, Mori H. 2006. Construction of *Escherichia coli* K-12 in-frame, single-gene knockout mutants: the Keio collection. Mol Syst Biol 2:2006 0008.

81 **Table S1.** List of *E. coli* strains

Strain [a]	Genotype [b]
MG1655	*E. coli* K-12 wild-type
MDS42	MG1655 with 42 engineered deletions in genome
GJ12134	MDS42 Δ(*argF-lac*)*U169*
GJ13519	MG1655 Δ(*argF-lac*)*U169* [ϕ80 lysogen]
GJ13531 [c]	GJ13519 Δ*rho*::Kan *att* λ::P_{tac} –UvsW (Amp^R)
GJ15603 [d]	GJ13519 Δ*topA*::Kan
GJ15604 [d]	GJ13519 *topA*-Ins480::Kan
GJ15630 [a]	GJ13519 *dnaA177* Δ*dgoT*::FRT *rpoB*35 btuB*::Tn*10 topA*-Ins480::FRT Δ*tus*::FRT
GJ15688 [d]	GJ13519 *topA*-480Δ::Kan
GJ15697 [d]	GJ15603 *att* λ::P_{tac} –UvsW (Amp^R)
GJ16475 [e]	GJ13519 *rpoB*35 btuB*::Tn*10* Δ*dnaA*:::FRT Δ*tus*::FRT Δ*rnhA*::FRT
GJ16703	GJ13519 *rpoB*35 btuB*::Tn*10*
GJ16813 [d]	GJ16703 Δ*topA*::Kan
GJ16814 [d]	GJ16703 *topA*-Ins480::Kan
GJ16815 [d]	GJ16703 *topA*-480Δ::Kan
GJ16816 [d]	GJ12134 Δ*topA*::Kan
GJ16817 [d]	GJ12134 *topA*-Ins480::Kan
GJ16818 [d]	GJ12134 *topA*-480Δ::Kan
GJ16819	GJ12134 *rpoB*35 btuB*::Tn*10*
GJ16820 [d]	GJ16819 Δ*topA*::Kan
GJ16821 [d]	GJ16819 *topA*-Ins480::Kan
GJ16822 [d]	GJ16819 *topA*-480Δ::Kan
GJ16854 [d]	GJ16703 *topA*-Ins480::FRT
GJ16880[d]	GJ16854 Δ*uvrD*::Kan
GJ16902 [d]	GJ12134 *rpoB*35 btuB*::Tn*10 dnaA177* Δ*dgoT*::FRT Δ*tus*::FRT Δ*topA*::FRT
GJ16903 [d]	GJ12134 *rpoB*35 btuB*::Tn*10 dnaA177* Δ*dgoT*::FRT Δ*tus*::FRT *topA*-Ins480::FRT
GJ16904[d]	GJ12134 *rpoB*35 btuB*::Tn*10 dnaA177* Δ*dgoT*::FRT Δ*tus*::FRT *topA*-480Δ::FRT
GJ16921 [d]	GJ13519 *topA*-Ins480::FRT
GJ17776 [d]	GJ16819 Δ*topA*::FRT
GJ17777 [d]	GJ16819 *topA*-Ins480::FRT
GJ17778 [d]	GJ16819 *topA*-480Δ::FRT

GJ17783 [d]	GJ13519 Δ*tus*::FRT *rpoB*35 btuB*::Tn*10* Δ*topA*::FRT
GJ17784 [d]	GJ13519 Δ*tus*::FRT *rpoB*35 btuB*::Tn*10 topA*-Ins480::FRT
GJ17786 [d]	GJ17783 Δ*dnaA*::Kan
GJ17787 [d]	GJ17784 Δ*dnaA*::Kan
GJ17788 [d]	GJ13519 Δ*tus*::FRT *rpoB*35 btuB*::Tn*10 topA*-480Δ::FRT Δ*dnaA*::Kan
GJ17789 [d]	GJ13519 Δ*tus*::FRT *rpoB*35 btuB*::Tn*10* Δ*dnaA*::FRT
GJ17790 [d]	GJ17789 Δ*topA*::Kan
GJ17791 [d]	GJ17789 *topA*-Ins480::Kan
GJ17792 [d]	GJ17789 *topA*-480Δ::Kan
GJ18601	GJ13519 ϕ80 free
GJ18904 [d]	GJ17776 Δ*dnaA*::FRT
GJ18905 [d]	GJ17777 Δ*dnaA*::FRT
GJ18906 [d]	GJ17778 Δ*dnaA*::FRT
GJ18907 [d]	GJ18904 Δ*tus*::Kan
GJ18908 [d]	GJ18905 Δ*tus*::Kan
GJ18909 [d]	GJ18906 Δ*tus*::Kan
GJ18910	GJ18601 *rpoB*35 btuB*::Tn*10*
GJ18918 [d]	GJ18910 *topA*-Ins480::FRT
GJ18921 [d]	GJ18918 Δ*dinG*::Kan
GJ18940 [d]	GJ17783 Δ*dnaA*::FRT
GJ18941 [d]	GJ17784 Δ*dnaA*::FRT
GJ18942 [d]	GJ13519 Δ*tus*::FRT *rpoB*35 btuB*::Tn*10 topA*-480Δ::FRT Δ*dnaA*::FRT
GJ18945 [d]	GJ18918 Δ*tus*::Kan
GJ18951 [d]	GJ18941 Δ*rnhA*::Kan
GJ18952 [d]	GJ18941 Δ*dinG*::Kan
GJ18976 [d]	GJ12134 Δ*topA*::FRT
GJ18977 [d]	GJ12134 *topA*-Ins480::FRT
GJ18983 [d]	GJ18940 Δ*rnhA*::Kan
GJ18997 [d]	GJ13519 *dnaA177* Δ*dgoT*::FRT *rpoB*35 btuB*::Tn*10* Δ*tus*::FRT Δ*topA*::FRT
GJ18999 [d]	GJ13519 *dnaA177* Δ*dgoT*::FRT *rpoB*35 btuB*::Tn*10* Δ*tus*::FRT *topA*-480Δ::FRT
GJ19608 [d]	GJ17783 Δ*rnhA*::Kan
GJ19609 [d]	GJ17784 Δ*rnhA*::Kan

82

83 [a] Strain MG1655 was from our laboratory collection. Strains MDS42 (3),
84 GJ12134 (4), GJ13519 (1), GJ13531 (5), and GJ16475 (1) have been
85 described earlier; all other strains were constructed in this study.

86 [b] The following alleles and constructs have been described earlier: Δ(*argF-*
87 *lac)U169* (6); *dnaA177* (7); Keio deletions of *rnhA*, *tus*, *dinG*, *dgoT*, *uvrD*, and
88 *tus* (8); *rpoB*35* and *btuB*::Tn*10* (1); and att λ::P_{tac}–UvsW(Amp^r) (4).

89 [c] Strain GJ13531 was routinely maintained as derivative with the shelter
90 plasmid pHYD2411.

91 [d] The indicated strains were routinely maintained as derivatives with the
92 shelter plasmid pHYD2390.

93 [e] Strain GJ16475 was routinely maintained as derivative with the shelter
94 plasmid pHYD2388.

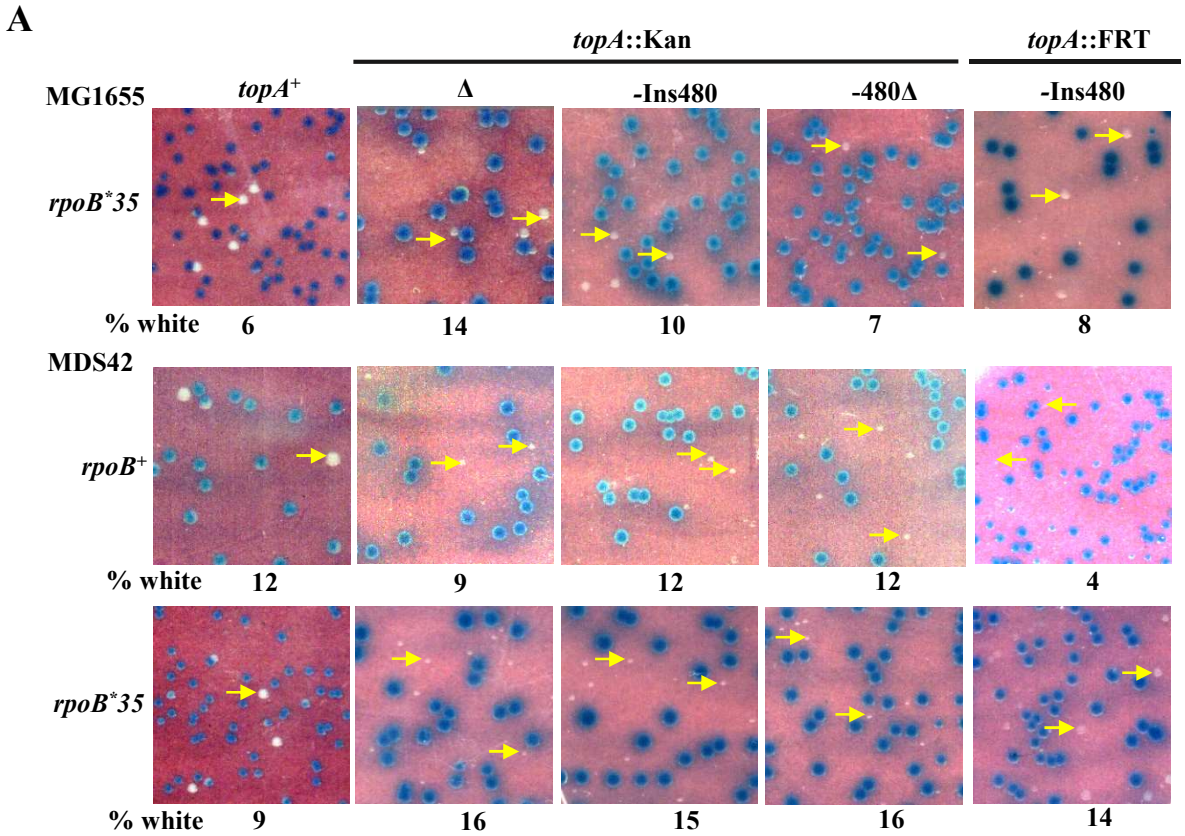

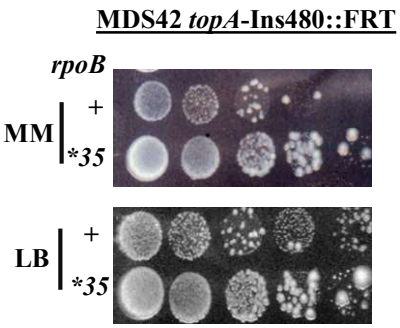

Supplementary Figure S1. (A) Blue-white screening assay on glucose-minimal A medium, of MG1655 or MDS42 strain derivatives with the *topA*$^+$ shelter plasmid pHYD2390 and the different *topA* alleles as indicated on the top of each column; the *rpoB* allele status is indicated at left of each row. Examples of white colonies are marked by the yellow arrows. From left to right, strains used for the panels were pHYD2390 derivatives of: row 1, GJ16703, GJ16813, GJ16814, GJ16815 and GJ16854; row 2, GJ12134, GJ16816, GJ16817, GJ16818 and GJ 18977; and row 3, GJ16819, GJ16820, GJ16821, GJ16822 and GJ17777. **(B)** Serial dilution-spotting of *rpoB*$^+$ and *rpoB*35* derivatives of MDS42 *topA*-Ins480::FRT (GJ18977 and GJ17777, respectively) on LB and MM.

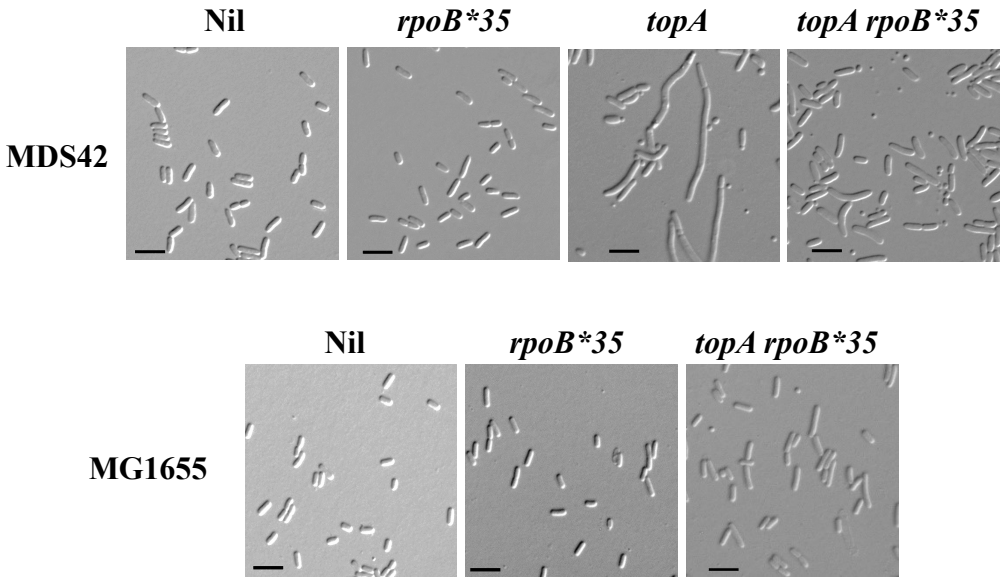

Supplementary Figure S2. Cell morphology in derivatives of MDS42 and MG1655 (top and bottom rows, respectively), visualized by differential interference contrast microscopy. Scale bar (at bottom left of each panel), 5 μm. Relevant mutations in the strains are indicated on top of the corresponding panels. The *topA* allele in MDS42 derivatives was Δ*topA*::Kan and that in the MG1655 derivative was *topA*-Ins480::Kan. Strains used were (from left to right): top row, GJ12134, GJ16819, GJ16816, and GJ16820; and bottom row, GJ13519, GJ16703, and GJ16814.

A

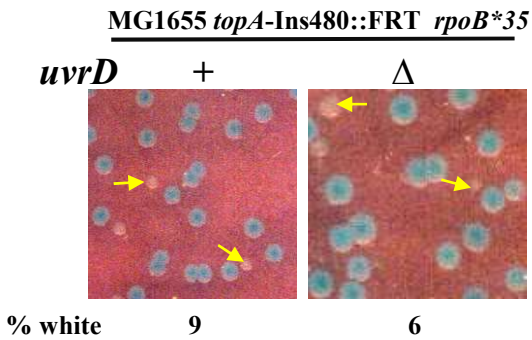

B

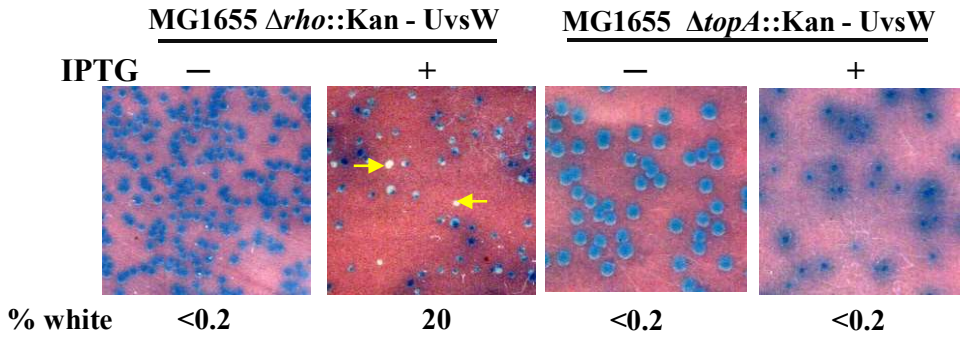

Supplementary Figure S3. Blue-white screening assays with MG1655 derivatives (carrying cognate shelter plasmids) on glucose-minimal A medium to demonstrate that *topA* lethality rescue by *rpoB*35* is UvrD-independent **(A)**, and that UvsW expression rescues Δ*rho* lethality but not Δ*topA* lethality **(B)**. Relevant genotypes are indicated on top of each of the panels. Examples of white colonies are marked by the yellow arrows. UvsW expression from a chromosomal P_{tac}-UvsW construct was regulated by the omission (−) or addition (+) of IPTG (latter at 100 µM and 40 µM, respectively, for the *rho* and *topA* mutants). Strains used were: **(A)** pHYD2390 derivatives of GJ16854 (*uvrD*$^{+}$) and GJ16880 (Δ*uvrD*); and **(B)** pHYD2411 derivative of GJ13531 (Δ*rho*) and pHYD2390 derivative of GJ15697 (Δ*topA*).

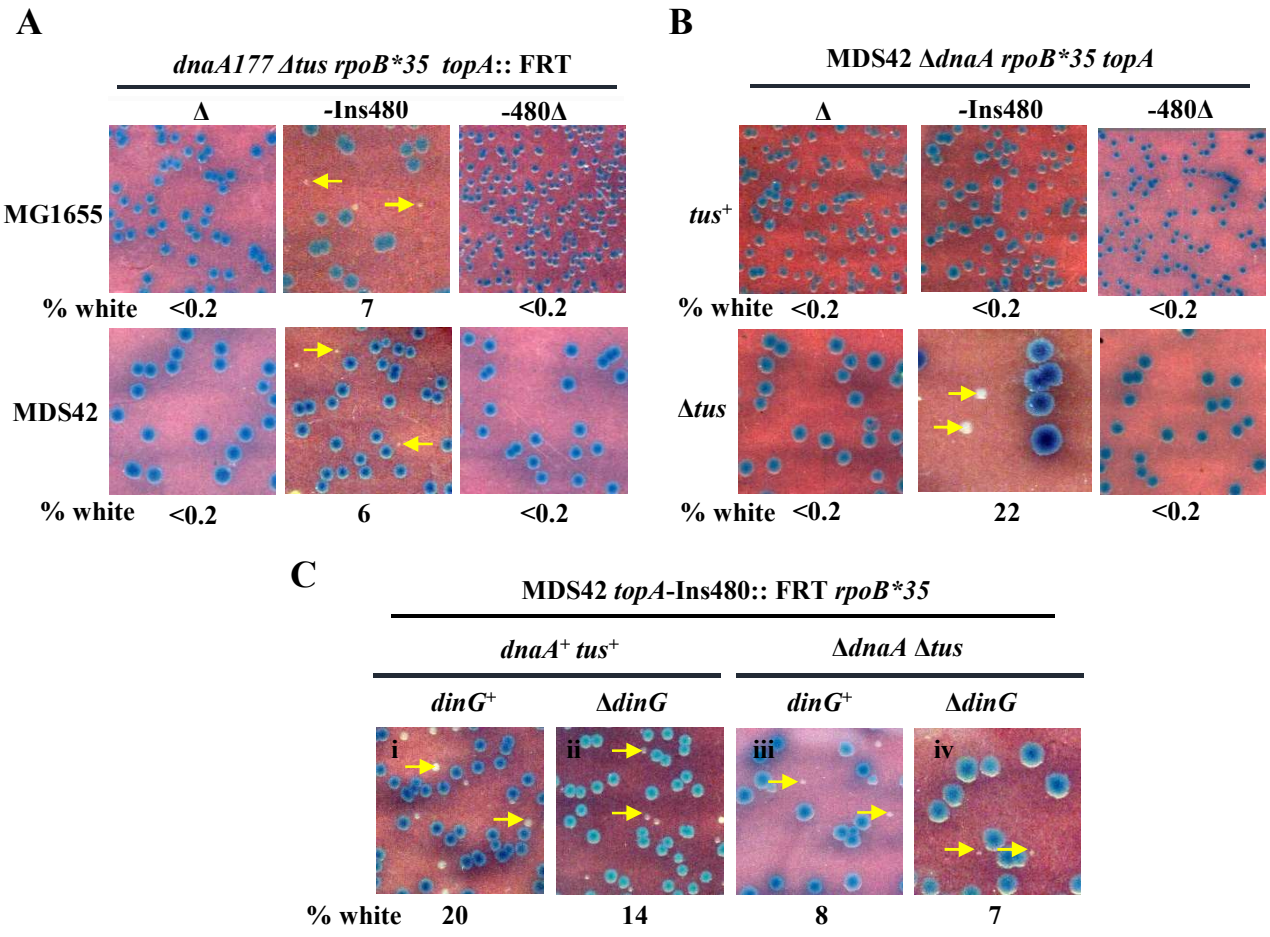

Supplementary Figure S4. Features of *dnaA* lethality rescue by *topA* alleles. **(A-C)** Blue-white screening assays were performed at 30° on glucose-minimal A with *topA*$^+$ *dnaA*$^+$ shelter plasmid pHYD2390 in strain derivatives of MG1655 or MDS42 whose relevant genotypes are indicated on top of each of the panels. Examples of white colonies are marked by the yellow arrows. From left to right, strains employed were pHYD2390 derivatives of: **A** top row, GJ18997, GJ15630 and GJ18999; **A** bottom row, GJ16902, GJ16903 and GJ16904; **B** top row, GJ18904, GJ18905 and GJ18906; **B** bottom row, GJ18907, GJ18908 and GJ18909; and **C**, GJ18918, GJ18921, GJ18941 and GJ18952.

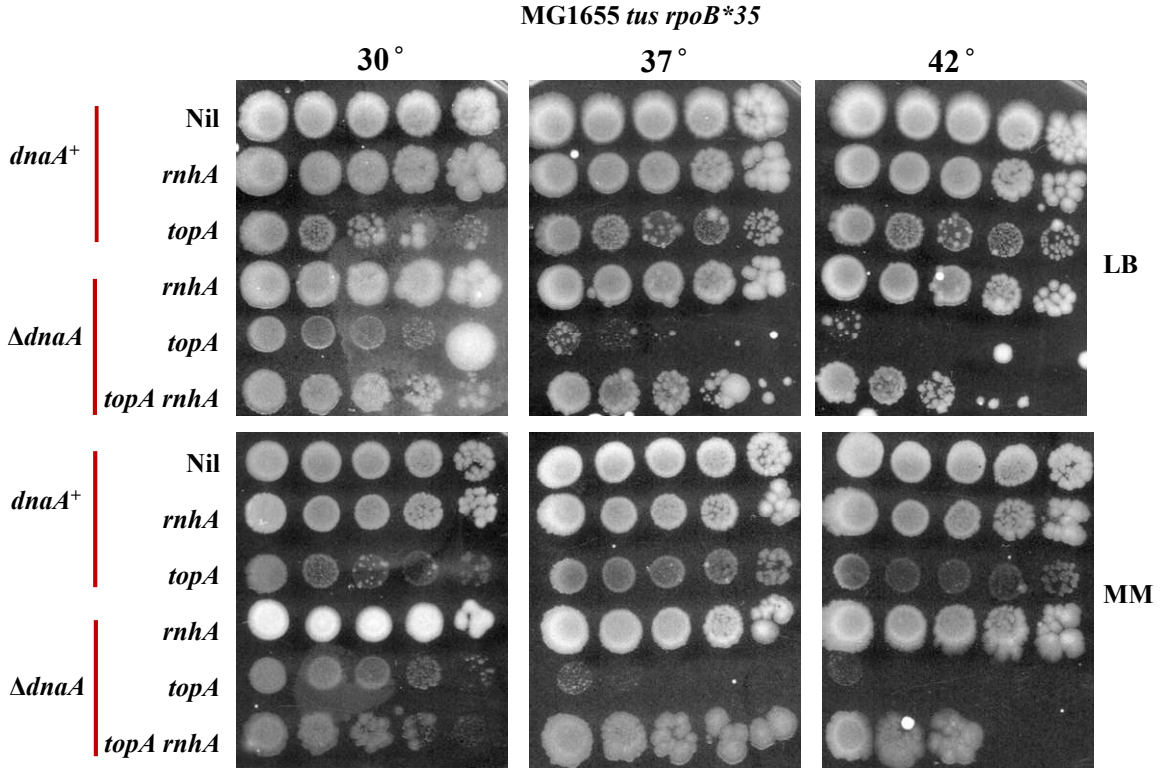

Supplementary Figure S5. Serial dilution-spotting on LB and glucose-minimal A (MM) at indicated temperatures of derivatives of MG1655 Δ*tus rpoB*35* with additional relevant alleles as indicated at left. The Δ*dnaA*, *topA* and *rnhA* alleles were, respectively, Δ*dnaA*::FRT, *topA*-Ins480::FRT, and Δ*rnhA*::Kan. The six strains used were (from top): GJ17784/pHYD2390; GJ16475/pHYD2388; GJ17784; GJ16475; GJ18941; and GJ18951.

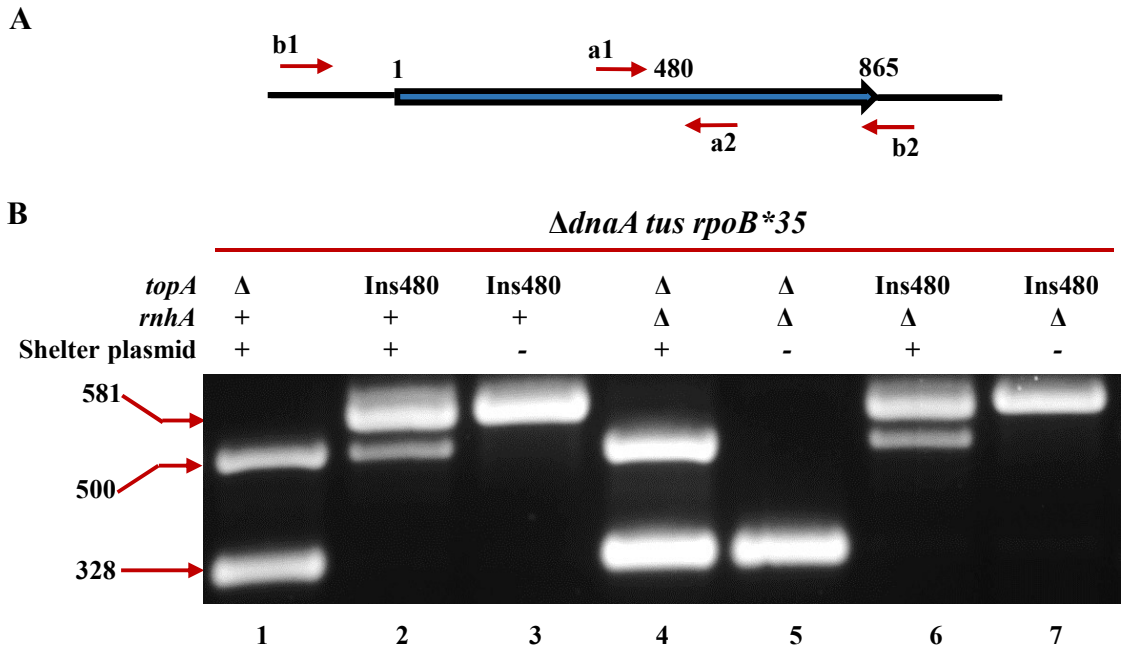

Supplementary Figure S6. PCR validation of chromosomal *topA* genotype in Δ*dnaA* derivatives without or with *rnhA* mutation. **(A)** Schematic depiction of *topA* ORF (865 codons); positions of PCR primer pairs a1-a2 (5'-TGTACCAGTTAATCTGGCGTCAG-3' and 5'-TCGTGATTTGCCACCTGGTCGAG-3', respectively) flanking the codon 480 region, and b1-b2 (sequences given in Supplementary Methods above) for the entire ORF, are marked. The former primer pair is expected to yield amplicons of size 500 bp and 581 bp from *topA*$^+$ and *topA*-Ins480::FRT, respectively, and no amplicon from Δ*topA*::FRT. The latter primer pair is expected to yield amplicons of size 2.8 kb and 328 bp from *topA*$^+$ and Δ*topA*::FRT, respectively; however, the conditions used for PCR amplification were such as not to yield the large-size amplicons such as of 2.8 kb length. **(B)** Amplicons detected by gel electrophoresis after PCR with both primer pairs together, on DNA preparations from strains of genotype indicated on top of each lane. The *topA*$^+$ *dnaA*$^+$ shelter plasmid was pHYD2390. Allele designations used for *topA*: Δ, Δ*topA*::FRT and 480, *topA*-Ins480::FRT; and for *rnhA*: Δ, Δ*rnhA*::Kan. Migration positions of fragments of length 328, 500 and 581 bp are marked. Strains employed for the different lanes were: 1, GJ18940/pHYD2390; 2, GJ18941/pHYD2390; 3, GJ18941; 4, GJ18983/pHYD2390; 5, GJ18983; 6, GJ18951/pHYD2390; and 7, GJ18951.